

# Linear Optimal Low-Rank Projection for High-Dimensional Multi-Class Data

Joshua T. Vogelstein\*, Minh Tang, Eric Bridgeford, Da Zheng, Randal Burns, Mauro Maggioni

Johns Hopkins University

**Classifying samples into categories becomes intractable when a single sample can have millions to billions of features, such as in genetics or imaging data. Principal Components Analysis (PCA) is widely used to identify a low-dimensional representation of such features for further analysis. However, PCA ignores class labels, such as whether or not a subject has cancer, thereby discarding information that could substantially improve downstream classification performance. We describe an approach, “Linear Optimal Low-rank” projection (LOL), which extends PCA by incorporating the class labels in a fashion that is advantageous over existing supervised dimensionality reduction techniques. We prove, and substantiate with synthetic experiments, that LOL leads to a better representation of the data for subsequent classification than other linear approaches, while adding negligible computational cost. We then demonstrate that LOL substantially outperforms PCA in differentiating cancer patients from healthy controls using genetic data, and in differentiating gender using magnetic resonance imaging data with >500 million features and 400 gigabytes of data. LOL therefore allows the solution of previous intractable problems, yet requires only a few minutes to run on a desktop computer.**

Supervised learning—the art and science of estimating statistical relationships using labeled training data—has enabled a wide variety of basic and applied findings, ranging from discovering biomarkers in omics data [1] to recognizing objects from images [2]. A special case of supervised learning is classification; a classifier predicts the “class” of a novel observation, for example, by predicting sex from an MRI scan. One of the most foundational and important approaches to classification is Fisher’s Linear Discriminant Analysis (LDA) [3]. LDA has a number of highly desirable properties for a reference classifier. First, it is based on simple geometric reasoning: when the data are Gaussian, all the information is in the means and variances, so the optimal classifier uses both the means and the variances. Second, due to its simplicity, LDA can be applied to multiclass problems. Third, theorems guarantee that when the sample size  $n$  is large and the dimensionality  $p$  is small, LDA converges to the optimal classifier under the Gaussian assumption. Finally, partially because of its simplicity, algorithms for implementing it are highly efficient.

Modern scientific datasets, however, present challenges for classification that were not addressed in Fisher’s era. Specifically, the dimensionality of datasets is quickly ballooning. Current raw data can consist of hundreds of millions of features or dimensions; for example, an entire genome or connectome. Yet, the sample sizes have not experienced a concomitant increase. This “large  $p$ , small  $n$ ” problem is a non-starter for many classical statistical approaches because they were designed with a “small  $p$ , large  $n$ ” situation in mind. LDA in particular estimates a hyperplane in  $p - 1$  dimensions when the data are  $p$  dimensional. When  $n$  is as large as  $p$ , this is akin to fitting a plane to two points: there are an infinite number of choices. Therefore, without further constraints, algorithms will “overfit”, meaning will learn a classifier including the noise in the data, rather than discarding the noise in favor of the desired signal. Supervised manifold learning is a field devoted to combating this overfitting issue by searching for a small number of dimensions that maximize predictive accuracy.

Three complementary strategies have been pursued to overcome this overfitting. Perhaps the most widely used is Principal Components Analysis (PCA) [4]. PCA “pre-processes” the data by reducing its dimensionality to those dimensions whose variance is largest in the dataset. While highly successful,

PCA is a wholly unsupervised dimensionality reduction technique, meaning that PCA does not use the class labels while learning the low-dimensional representation. This approach results in dimensions that have no statistical guarantee of being close to the best ones for classification. In fact, we show below that there is a high probability that the resulting classifier will operate at chance levels in some circumstances. Another unsupervised nonlinear dimensionality reduction approach, called manifold learning [5], is ill-equipped to address this problem because such approaches typically only learn a low-dimensional representation for the data at hand, rather than all potential data points, and therefore cannot be applied to new test data. Moreover, manifold learning often requires costly numerical methods that do not scale well, and lack theoretical justification in this setting.

A second strategy used to overcome overfitting is to regularize or penalize a supervised method, such as LDA [6] or canonical correlation analysis (CCA) [7]. “Truncated” variants of LDA and CCA are designed to keep the dimensions that are most informative with regard to the task at hand. However, as we demonstrate below, both approaches are problematic in the  $n \leq p$  setting of interest here. We also demonstrate that Partial Least Squares (PLS) has the same drawbacks as CCA [?].

Sparse methods are the third common strategy to mitigate this “curse of dimensionality”. Sparse methods find a small subset of the original features to use for subsequent inference [8]. The advantage of sparse methods is that their results are sometimes more interpretable than those obtained with PCA-based methods. The disadvantage, however, is that the time required to exactly solve sparse problems increases exponentially with the number of features, making exact approaches intractable for large high-dimensional datasets. Various approximations for sparse methods enable efficient algorithms with convergence guarantees under certain limiting assumptions. Lasso is a particularly popular algorithm of this sort [9]. Unfortunately, has some hyper-parameters that requires careful tuning, and can produce spurious answers even when its unrealistically strict assumptions are met [10]. A more recent sparse method is called “regularized optimal affine discriminant” (ROAD) [11]. ROAD finds the optimal sparse dimensions under certain Gaussian assumptions. ROAD, however, can only be applied in two-class settings, and requires solving a computationally costly numerical optimization problem, so it does not scale to large dimensionality.

Moreover, none of the above strategies have implementations that scale to millions or billions of features. Instead, recent big data packages are designed for millions or billions of samples [12, 13]. In biomedical sciences, however, it is far more common to have tens or hundreds of samples, and millions or billions of features (e.g., genomics or connectomics). Thus, there is a gap for an approach that can classify multi-class data with millions of features, with strong theoretical guarantees, favorable empirical performance, and an efficient and scalable implementation.

To address these issues, we developed “Linear Optimal Low-rank” projection (LOL). The key intuition behind LOL is that we can jointly use both the class labels and the covariance to find low-dimensional representations, much like LDA and CCA, but without requiring more dimensions than samples, much like PCA, or restrictive sparsity assumptions, like ROAD. Using random matrix theory, we are able to prove that when the data are sampled from a Gaussian, LOL finds a better low-dimensional representation than PCA and supervised linear methods. Under certain relatively relaxed assumptions, this is true regardless of the dimensionality of the features, the number of samples, and the number of dimensions in which we project. We then demonstrate the superiority of LOL over other methods with both synthetic and experimental datasets.

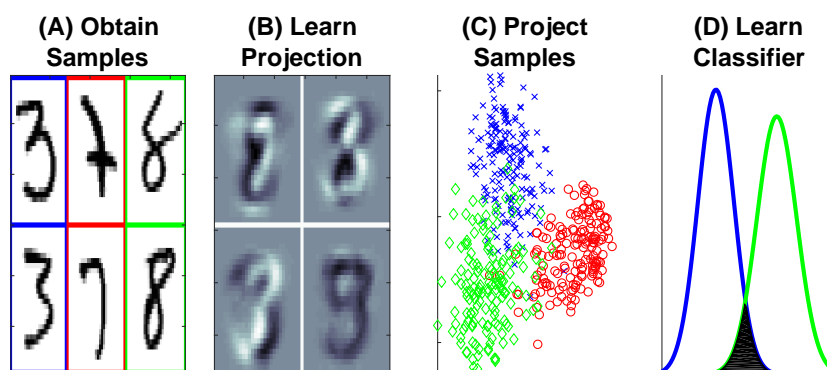


**Figure 1:** Schematic illustrating Linear Optimal Low-rank (LOL) as a supervised manifold learning technique. **(A)** 300 training samples of the numbers 3, 7, and 8 from the MNIST dataset (100 samples per digit); each sample is a  $28 \times 28 = 784$  dimensional image (boundary colors are for visualization purposes). **(B)** The first four projection matrices learned by LOL. Each is a linear combination of the sample images. **(C)** Projecting 500 new (test) samples into the top two learned dimensions; digits color coded as in (A). LOL-projected data form three distinct clusters. **(D)** Using the low-dimensional data to learn a classifier. The estimated distributions for 3 and 8 of the test samples (after projecting data into two dimensions and using LDA to classify) demonstrate that 3 and 8 are easily separable by linear methods after LOL projections (the color of the line indicates the digit). The filled area is the estimated error rate; the goal of any classification algorithm is to minimize that area. LOL is performing well on this high-dimensional real data example.

## Supervised Manifold Learning

A general strategy for supervised manifold learning is schematized in Figure 1. Step **(A)**, obtain or select  $n$  training samples of high-dimensional data. For concreteness, we use one of the most popular benchmark datasets, the MNIST dataset [14]. This dataset consists of images of hand-written digits 0 through 9. Each such image is represented by a  $28 \times 28$  matrix, which means that the observed dimensionality of the data is  $p = 28^2 = 784$ . Because we are motivated by the  $n \ll p$  scenario, we subsample the data to select  $n = 300$  examples of the numbers 3, 7, and 8 (100 of each). Step **(B)**, learn a “projection” that maps the high-dimensional data to a low-dimension representation. One can do so in a way that ignores which images corresponds to which digit (the “class labels”), as PCA and most manifold learning techniques do, or try to use the labels, as LDA and sparse methods do.<sup>1</sup> LOL is a supervised linear manifold learning technique, which uses the class labels to learn projections that are linear combinations of the original data samples. Step **(C)**, use the learned projections to map high-dimensional data into the learned lower-dimensional space. This step requires having learned a projection that can be applied to new (test) data samples for which we do not know the true class labels. Nonlinear manifold learning methods typically cannot be applied in this way (though see [15]). LOL, however, can project new samples in such a way as to separate the data into classes. Finally, step **(D)**, using the low-dimensional representation of the data, learn a classifier. A good classifier correctly identifies as many points as possible with the correct label. When LDA is used on the low-dimensional data learned by LOL, the data points are mostly linearly separable, yielding a highly accurate classifier.

<sup>1</sup>Linear dimensionality reduction techniques are said to learn a “projection” into a lower-dimensional space, whereas nonlinear methods are typically said to learn an “embedding”.

## Linear Gaussian Intuition

To build intuition for situations when LOL performs well, and when it does not, we consider the simplest high-dimensional classification setting. We observe  $n$  samples  $(\mathbf{x}_i, y_i)$ , where  $\mathbf{x}_i$  are  $p$  dimensional feature vectors, and  $y_i$  is the binary class label, that is  $y_i$  is either 0 or 1. We assume that both classes are distributed according to a multivariate Gaussian distribution, the two classes have the same covariance matrix  $\Sigma$ , and data from either class is equally likely, so that the only difference between the classes is their means,  $\mu^1$  and  $\mu^2$ . The optimal low-dimensional projection is analytically available in this scenario—commonly referred to as Fisher’s Linear Discriminant Analysis (LDA)—it is the dot product of the difference of means and the inverse covariance matrix,  $(\mu^1 - \mu^2)^\top \Sigma^{-1}$  [16] (see Appendix A for derivation). When the distribution of the data is unavailable, as in all real data problems, machine learning methods can be used to estimate the parameters. Unfortunately, when  $n < p$ , the estimated covariance matrix will not be invertible (because the solution to the underlying mathematical problem is under specified), so some other approach is required. As mentioned above, PCA is commonly used to learn a low-dimensional representation. Formally, PCA uses the pooled sample mean,  $\hat{\mu} = \frac{1}{n} \sum_{i=1}^n \mathbf{x}_i$  and the pooled sample covariance matrix,  $\hat{\Sigma}$  with entries  $\hat{\Sigma}_{kl} = \frac{1}{n} \sum_{i=1}^n (x_{ik} - \hat{\mu}_k)(x_{il} - \hat{\mu}_l)$ . The PCA projection is composed of the top  $d$  eigenvectors of the pooled sample covariance matrix, so it completely ignores the class labels.

In contrast, LOL uses the class-conditional means and class-conditional covariance. This approach is motivated by Fisher’s LDA, which uses the same two terms, and should therefore improve performance over PCA, which uses the pooled estimates rather than the class-conditional estimates. More specifically, for a two-class problem, LOL first computes the sample mean of each class,  $\hat{\mu}^j = \frac{1}{n_j} \sum_{i:y_i=j} \mathbf{x}_i$ , where  $n_j$  is the number of samples in class  $j$ . Second, LOL estimates the difference between means,  $\hat{\delta} = \hat{\mu}^1 - \hat{\mu}^2$ . Third, LOL computes the class-conditional covariance matrix,  $\tilde{\Sigma}$  with entries  $\tilde{\Sigma}_{kl} = \frac{1}{2} \sum_{j=1}^J \frac{1}{n} \sum_{i:y_i=j} (x_{ik} - \mu_k^j)(x_{il} - \mu_l^j)$ . In other words, LOL centers each data point with respect to the mean of its own class, rather than the overall pooled mean, and then computes the class-centered covariances. Fourth, LOL computes the eigenvectors of this class-conditionally centered covariance: these eigenvectors correspond to the directions that maximize the variance after subtracting the class-conditional means. If one does not subtract these means, the directions that maximize variance will point towards the means, which are already accounted for by the mean computation. Finally, LOL simply concatenates the difference of the means with the top  $d - 1$  eigenvectors of  $\tilde{\Sigma}$ . Note that the sample class-conditional covariance matrix estimates the population covariance,  $\Sigma$ , whereas the sample pooled covariance matrix is distorted by the difference of the class means. For the theoretical background on LDA, a formal definition of LOL, and detailed description of the simulation settings that follow, see Appendices A, B, and C, respectively.

Figure 2 shows three different examples of data sampled from the Gaussian model to geometrically illustrate the intuition that motivated LOL. In each, the top row shows, for  $n = 100$  training samples, the first two dimensions of a  $p = 1000$  dimensional space, so  $n \ll p$ . The next four rows each show the distribution of test data after using LDA on the low-dimensional representation.

Figure 2A shows an example we call “stacked cigars”. In this example, all dimensions are uncorrelated with one another. Moreover, (1) the difference between the means and (2) the direction of maximum variance are both large along the same dimensions. This is an idealized setting for PCA, because PCA finds the direction of maximal variance, which happens to correspond to the direction of maximal separation of the classes. We also compare this to a method which projects the data onto top  $d$  eigenvectors of the sample class-conditional covariance matrix,  $\tilde{\Sigma}$  after centering using the pooled mean. Composing this projection with LDA is equivalent to a method called “Reduced Rank LDA” [17] (see

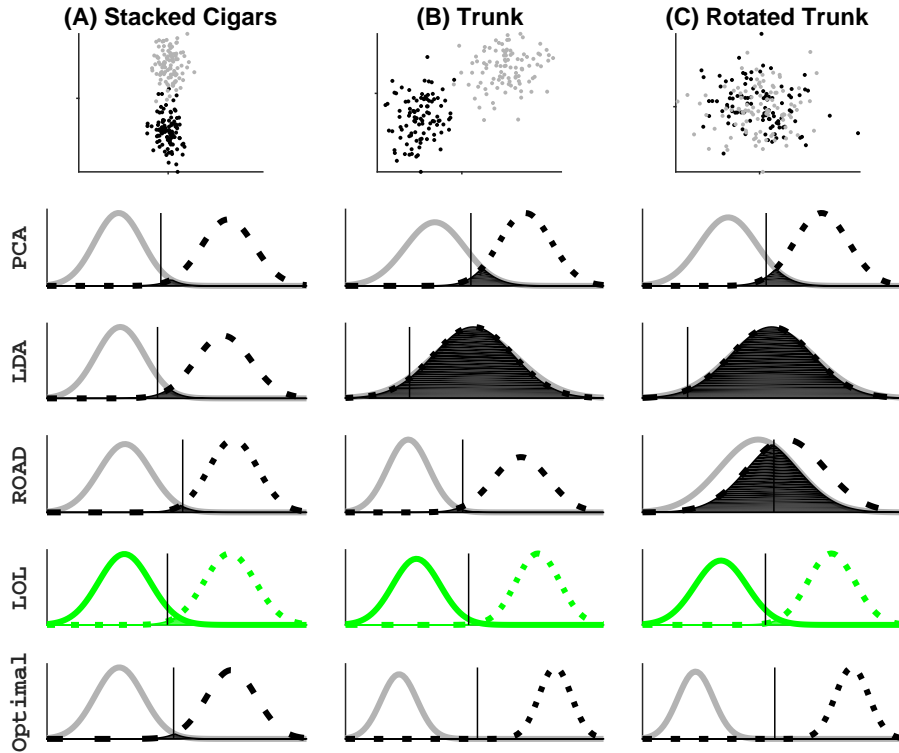


**Figure 2:** LOL achieves near-optimal performance for a wide variety of Gaussian distributions. Each point is sampled from a multivariate Gaussian; the three columns correspond to different simulation parameters. In each of three simulations, we sample  $n = 100$  points in  $p = 1000$  dimensions, so  $n \ll p$ . And for each approach, we project into the top 3 dimensions, and then used LDA to find the one-dimensional projection. Note that we use the sample estimates, rather than the true population values of the parameters. The six rows show (from top to bottom): **Row 1:** A scatter plot of the first two dimensions of the sampled points, with class 0 and 1 as black and gray dots, respectively. The next rows each show estimates of the two class-conditional posteriors resulting from projecting the data using different manifold learning techniques, including PCA (**Row 2**); LDA, a method that projects onto the top  $d$  eigenvectors of sample class-conditional covariance (**Row 3**); ROAD, a sparse method designed specifically for this model (**Row 4**); LOL, our proposed method (**Row 5**); the Bayes optimal classifier (**Row 6**). In each case, the solid (dashed) line is the estimated posterior for class 0 (class 1), and the overlap of the distributions—which quantifies the magnitude of the error—is filled. The black vertical line shows the estimated threshold for each method. **(A)** The mean difference vector is aligned with the direction of maximal variance, and is mostly concentrated in a single dimension, making it ideal for PCA, LDA, and sparse methods. In this setting, the results are similar for all methods, and essentially optimal. **(B)** The mean difference vector is orthogonal to the direction of maximal variance, making PCA perform worse, LDA is at chance, but sparse methods and LOL can still recover the correct dimensions, achieving nearly optimal performance. **(C)** Same as B, but the data are rotated, in this case, only LOL performs well. Note that LOL is closest to Bayes optimal in all three settings.

Appendix II.B for proof); we therefore refer to this approach as LDA hereafter. LDA performs well here too, for the same reason that PCA does. Because all dimensions are uncorrelated, and one dimension contains most of the information discriminating between the two classes, this is an ideal scenario for sparse methods. Indeed, ROAD, a sparse classifier designed for precisely this scenario, does an ex-

cellent job finding the most useful dimensions [11]. LOL, using both the difference of means and the directions of maximal variance, also does well. To calibrate all of these methods, we also show the performance of the optimal classifier.

Figure 2B shows an example that is worse for PCA. In particular, the variance is getting larger for subsequent dimensions,  $\sigma_1 < \sigma_2 < \dots < \sigma_p$ , while the magnitudes of the difference between the means are decreasing with dimension,  $\delta_1 > \delta_2 < \dots > \delta_p$ . Because PCA operates on the pooled sample covariance matrix, the dimensions with the maximum difference are included in the estimate, and therefore, PCA finds some of them, while also finding some of the dimensions of maximum variance. The result is that PCA performs fairly well in this setting. LDA, however, by virtue of subtracting out the difference of the means, is now completely at chance performance. ROAD is not hampered by this problem; it is also able to find the directions of maximal discrimination, rather than those of maximal variance. Again, LOL, by using both the means and the covariance, does extremely well.

Figure 2C is exactly the same as Figure 2B, except the data have been randomly rotated in all 1000 dimensions. This means that none of the original features have much information, rather, linear combinations of them do. This is evidenced by observing the scatter plot, which shows that the first two dimensions fail to disambiguate the two classes. PCA performs even worse in this scenario than in the previous one. LDA is rotationally invariant (see Appendix II.D for details), so still performs at chance levels. Because there is no small number of features that separate the data well, ROAD fails. LOL performs nearly as well here as it does in the other examples.

Collectively, these three examples demonstrate situations in which, based purely on geometric intuition, LOL performs as expected in a variety of Gaussian settings.

## Statistical Theory Proving When LOL is Better than PCA and Other Supervised Linear Methods

The above numerical experiments provide the intuition to guide our theoretical developments.

**Main Result** LOL is always better than or equal to LDA under the Gaussian model when  $p \geq n$ , and better than or equal to PCA (and nearly any other linear projection) with additional (relatively weak) conditions. This is true for all possible observed dimensionalities of the data, and the number of dimensions into which we project, for sufficiently large sample sizes. Moreover, under relatively weak assumptions, these conditions almost certainly hold as the number of dimensions increases.

Formal statements of the theorems and proofs required to substantiate the above result are provided in Appendix D. The condition for LOL to be better than PCA is essentially that the  $d^{\text{th}}$  eigenvector of the pooled sample covariance matrix has less information about classification than the difference of the means vector. The implication of the above theorem is that it is better to incorporate the mean difference vector into the projection matrix than not under basically the same assumptions that motivate PCA. The degree of improvement is a function of the projection dimension  $d$ , the dimensionality of the feature set  $p$ , the number of samples  $n$ , and the parameters, but the existence of an improvement—or at least no worse performance—is independent of those factors.

It is worth specifying exactly what “better” means in this context. It is desirable to have a notion of better that is agnostic to the subsequent classifier, that is, a metric that quantifies how good a projection is, no matter which classifier is used. We used Chernoff Information to calculate the distance between the distributions after projection. Chernoff information is fundamentally related to the expected classification error; specifically, it is the exponential convergence rate for the Bayes error [18],

and therefore the tightest theoretical bound possible for this setting. The use of Chernoff information to theoretically evaluate the performance of an embedding strategy is novel, to our knowledge, and of independence interest.

## Numerical Experiments Extending Our Theoretical Results

Here we empirically investigate the performance of LOL using simulations, both under the model assumptions for which our theorems hold, as well as generalizations for which we currently lack theory. For each of the different scenarios, we sample  $n = 100$  training samples each with  $p = 100$  features; therefore, Fisher’s LDA cannot solve the problem because there are infinitely many ways to overfit. For each setting, we evaluate the misclassification rate on held-out data for all possible numbers of dimensions to project into. The comparison algorithms are PCA, LDA, CCA, and two sparse methods: Lasso [19] and ROAD [11]. ROAD is a sparse approach that was specifically designed for Gaussian data but only works for two-class problems, whereas Lasso was designed for finding sparse dimensions and can be applied to any number of classes.

**Theoretical model** We begin by investigating two scenarios that satisfy the LDA model assumptions required by our proofs. First, consider the trunk example from Figure 2B as well as a “Toeplitz” example, as depicted in Figures 3A and 3B, respectively. In both scenarios, for all dimensions, LOL achieves as low or lower error rate than other methods, often dramatically so, as predicted by theory. Note that while for Trunk both the mean and the covariance approximately sparse and therefore compressive, for Toeplitz, both are dense and not compressive.

**Multiple Classes** LOL can trivially be extended to  $> 2$  class situations, unlike ROAD. In brief, LOL computes the mean of each class, and then selects one mean to be the reference, and computes the difference between all the other means and the reference one. Under the linearity assumptions, this approach does not lose any information relative to computing the distance between all pairs of means (see Appendix B for details). We generated data again from the same Trunk example, but added a third class whose mean is the zero vector (Figures 3C). We used Lasso as the sparse method approach, which utterly fails in this near-sparse setting. As before, LOL outperforms the other methods for all dimensions.

**Fat Tails** Figure 3D shows a sparse example with “fat tails” to better mirror real data settings, which often have samples that are unlikely under the Gaussian model. More specifically, each class is the sum of multiple Gaussians, with the same mean, but different covariances. The qualitative results are consistent with those of the previous numerical experiments, even though we have no theoretical guarantees here. More specifically, LOL outperforms all other methods for all dimensions.

**QDA** It sometimes makes more sense to model each class as having a unique covariance matrix, rather than a shared covariance matrix. Assuming everything is Gaussian, the optimal classifier in this scenario is called Quadratic Discriminant Analysis (QDA) [20]. Intuitively then, we can modify LOL to compute the eigenvectors separately for each class, and concatenate them (sorting them according to their singular values). Moreover, rather than classifying the projected data with LDA, we can then classify the projected data with QDA (a procedure we refer to as Quadratic Optimal QDA, or QOQ). Indeed, simulating data according to such a model (Figure 3E), LOL performs slightly better than chance, regardless of the number of dimensions we use to project, whereas QOQ performs significantly better regardless of how many dimensions it keeps. This result demonstrates a straightforward generalization of LOL, available to us because of its simplicity and intuitiveness.

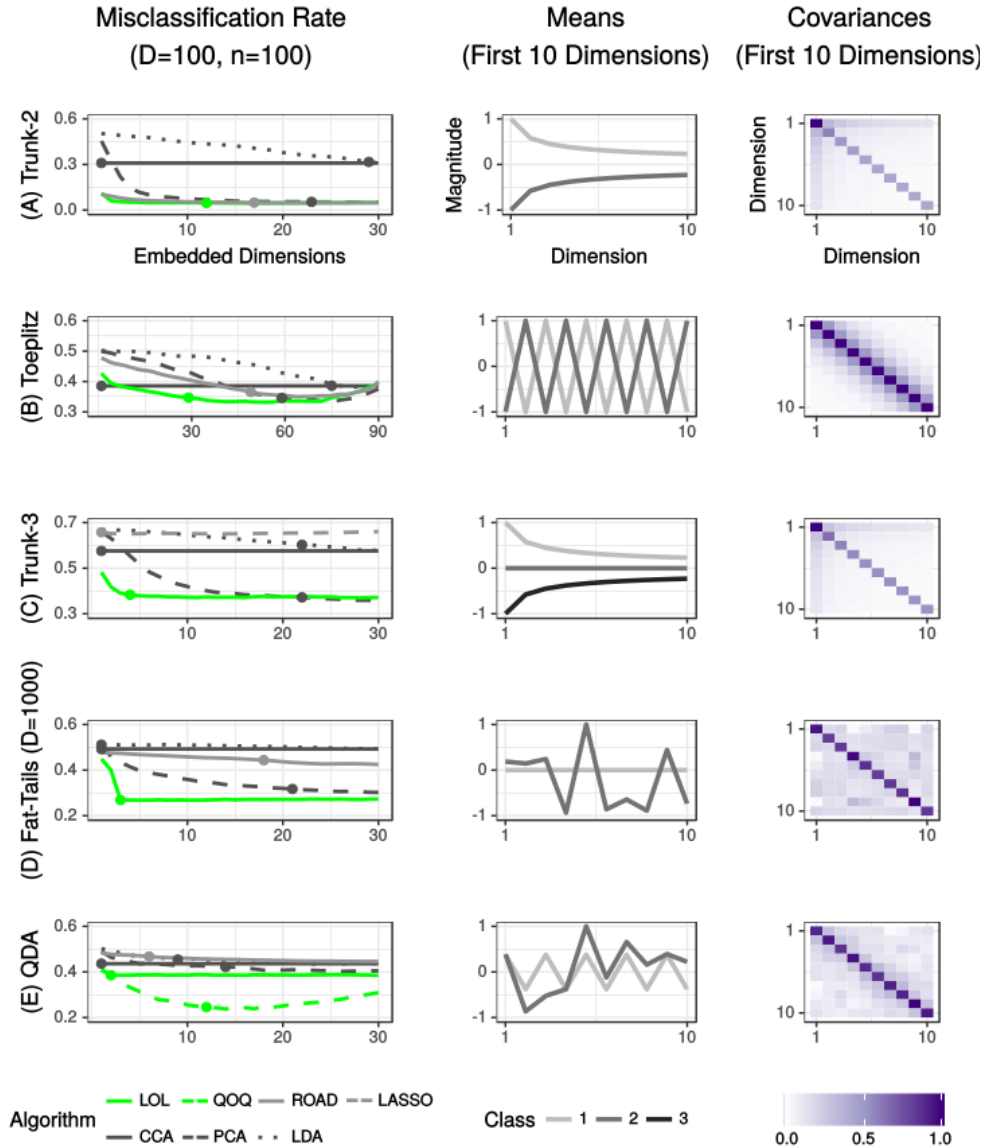


**Figure 3:** Five simulations demonstrating that LOL achieves superior finite sample performance over competitors, both in settings for which we have theoretical guarantees, and those for which we do not. For all cases,  $n = 100$  and  $p = 100$ , the left column depicts misclassification rate as a function of the number of projected dimensions, for several different approaches; the middle panels depict the first 10 dimensions of the means (different colors correspond to different classes); and the right panel depicts a the first 10 dimensions of the covariance matrix. The simulations settings are as follows: **(A)** Trunk-2: same as Figure 2C. **(B)** Toeplitz: another setting where mean difference is not well correlated with any eigenvector, and no ambient coordinate is particularly useful on its own. **(C)** Trunk-3: 3-class variant of the rotated Trunk example to demonstrate that LOL naturally adapts, and excels in, multi-class problems. **(D)** Fat Tails: a common phenomenon in real data that is more general than our theory supports; in this case dimensionality is 1000, which is 10-fold larger than the sample size. **(E)** QDA: QOQ, a variant of LOL when each class has a unique covariance, outperforms LOL, as expected, when the true discriminant boundary is a quadratic, rather than linear, function. In essentially all cases, LOL, or the appropriate generalization thereof, outperforms unsupervised or sparse methods for all dimensions, often by a large margin.

In all cases, both those for which theory supports the results, and those for which the simulations extend beyond our current theoretical understanding, LOL tends to achieve lower misclassification rate for any given dimension. In particular, low-rank CCA exhibits the “data piling problem”, where each sample from a given class is projected onto the exact same point, making the problem effectively one dimensional [21] (see Appendix IV.D for details). Thus, embedding CCA into higher dimensions is ineffective. Even the first dimension of CCA is worse than merely the difference of the means for four out of five of these simulations. For this reason, we do not pursue CCA further.

## Computational Efficiency

When the dimensionality  $p$  is large (e.g., millions or billions), the main bottleneck is sometimes merely the ability to run anything on the data, rather than its predictive accuracy. Fortunately, LOL has several algorithmic and implementation level properties that make it both flexible and computationally efficient. First, LOL admits a closed form solution, enabling it to leverage highly optimized linear algebra routines rather than the costly iterative programming techniques currently required for sparse or dictionary learning type problems [22]. Specifically, LOL is linear in both sample size and dimensionality (Figure 4A; light green line). Second, LOL is designed to be parallelizable. Typical parallelization strategies distribute work across compute nodes in a large cluster. However, doing so comes with a severe communication cost between the nodes. We therefore leverage recent advances in computer architecture, including multicore processors and solid-state drives. To empirically evaluate these claims, we simulated data using two classes of spherically symmetric Gaussians (see Appendix C for details) with dimensionality varying from 2 million to 128 million, and 1000 samples per class. This setting is ideal for PCA and LDA because the first principal component includes the mean difference vector.

Building on FlashX [23–25], we developed extremely efficient LOL implementations with an R interface for ease of use, including both an in-memory implementation when the data are small enough to be kept in RAM, and a semi-external memory implementation for larger data. Our implementations enable us to run LOL on essentially arbitrarily large data, achieving in-memory speeds for small data, and enabling the same speeds for multi-terabyte data (Figure 4A, dark green line). Third, because LOL is so simple, we can use randomized approximate algorithms to further accelerate its performance. In particular, random projections—for which the data are multiplied by a lower-dimensional random matrix—have been shown to provide excellent approximation eigenvectors [26]. Moreover, very sparse random projections, in which the elements of the matrix are mostly zero, with  $\pm 1$  randomly distributed, have been shown to be effective, and have significant computational benefits [27]. We therefore further modified FlashX to incorporate very sparse random projections, which we denote by Linear Fast Low-rank (LFL). LFL shows an order of magnitude improvement in both the in-memory and semi-external memory implementations (Figure 4A; orange lines); that is, rather than requiring 46 minutes on 128 million dimensional data, it requires 3 minutes. Importantly, the accuracy of LFL is essentially equivalent to LOL, at least in this simulated data (Figure 4B; green and orange lines). In contrast, LDA is barely performing better than chance, despite that the simulation is ideal for LDA.

These empirical observations mirror the theoretical bounds of performance. In particular, given  $T$  threads with sparsity  $c$ , our implementation has a computational complexity of  $\mathcal{O}(npd/Tc)$ , achieving the theoretically optimal speed up (as evidenced by the fact that the lines in Figure 4A are all straight and not asymptoting) and scale up (not shown).

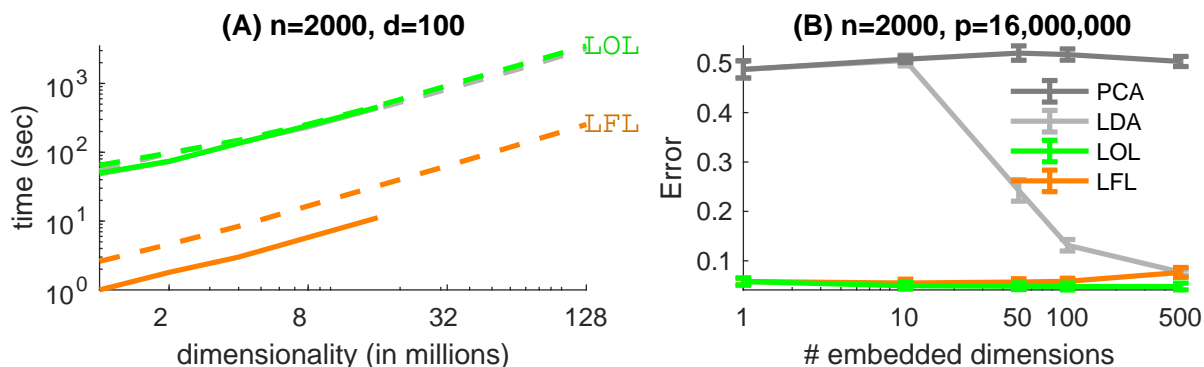


**Figure 4:** Computational efficiency of various low-dimensional projection methods. In all cases,  $n = 2000$ , and we used spherically symmetric Gaussians (see Appendix C for details). We compare PCA with LOL (solid green for in-memory, dashed green for semi-external memory), LFL (solid orange for in-memory, dashed orange for semi-external memory), and PCA (gray) for different observed dimensions. **(A)** LOL exhibits optimal (linear) scale up, requiring only 46 minutes to find the projection on a 2 terabyte dataset, and only 3 minutes using LFL. **(B)** Error for LFL is the same as LOL in this setting, and both are significantly better than PCA and LDA for all choices of projection dimension.

## Benchmark Real Data Applications

Real data often break the theoretical assumptions in more varied ways than the above simulations, and can provide a complementary perspective on the performance properties of different algorithms. We have therefore selected three high-dimensional datasets to compare LOL to several state-of-the-art algorithms (Figure 5, see Methods for details). For each dataset, we compare LOL to PCA, LDA, Lasso, and for the two-class problems, ROAD. For LOL, PCA, and LDA, we used Fisher’s LDA to classify the points after projecting into a lower-dimensional space.

Figure 5A shows performance on a commonly used two-class genetics dataset for sparse methods, with 2000 features and only 41 samples. Even though LOL is not a sparse method, it achieves a better (lower) misclassification rate than both sparse approaches, as well as PCA and LDA, using a leave-one-out strategy. Figure 5B shows performance on the MNIST dataset, which provided an illustration above. To challenge the methods, we only provided 100 samples total from the 10 classes, where each point is a 784 dimensional vector obtained from a  $28 \times 28$  dimensional image. PCA does nearly as well as LOL on this dataset, whereas the other methods perform substantially worse. By virtue of sub-sampling, we conducted this experiment 100 times using held-out data.

Finally, Figure 5C shows the performance of LOL on a dataset derived from diffusion magnetic resonance imaging. Specifically, we registered the raw data to a standard template (MNI152), and did no further pre-processing. This result is in stark contrast to the standard approaches to dealing with this data, which includes a deep processing chain, including many steps of parametric modeling and down-sampling [28–30]. At the native resolution, each brain volume is over 500 million dimensions, and we have only 112 samples, comprising over 400 gigabytes of data. We learned classifiers on the basis of sex, and evaluated using a leave-one-out procedure. As in the other two applications, LOL achieve a lower misclassification rate for all numbers of projection dimensions than both PCA and LDA. Neither ROAD nor Lasso can run on these big data, whereas using our fast approximate, out-of-core implementation of LOL, learning the embedding on this dataset only required a few minutes on a single computer. The minimum misclassification rate achieved via LOL is about 15%, which is the same per-

formance we and others obtain using extensively processed and downsampled data that is typically required on similar datasets [31, 32]. Details for exactly how to process these data remains controversial [33], so we side-step those issues by not processing and simply apply state-of-the-art machine learning to them.

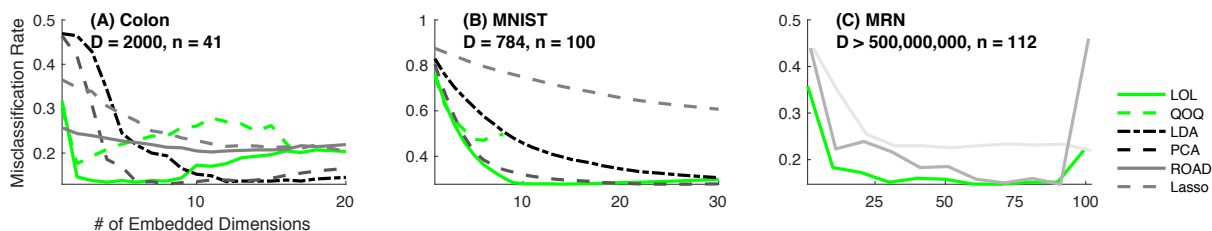


**Figure 5:** For three datasets, we benchmark LOL (green) versus standard classification methods, LDA (cyan), PCA (magenta), ROAD (orange), and Lasso (dark blue). For LOL, PCA, and LDA, we compose the projection with Fisher’s LDA. The three panels show the misclassification rate (vertical axis) and the number of projection dimensions (horizontal axis). (A) and (C) use leave-one-out misclassification rate to estimate error, whereas (B) had sufficient data to use held out data. Errorbars indicate standard error in each panel. **(A)** A standard sparse colon cancer genetics dataset. **(B)** A dense image dataset from Figure 1, but this time using all 10 digits. **(C)** A magnetic resonance imaging dataset with over five hundred million features. When using LDA to find a low-dimensional embedding, the result becomes numerically unstable when the number of dimensions approaches the number of samples, resulting in its performance to jumping up to chance levels. In all cases, for all number of projection dimensions, LOL does as well or better than all other methods.

## Discussion

We have introduced a very simple methodology to improve performance on supervised learning problems with wide data (that is, big data where dimensionality is as large or much larger than sample size). In particular, LOL uses both the difference of the means, and the covariance matrices, which enables it to outperform PCA in a wide variety of scenarios without incurring any meaningful additional computational cost. Our implementation optimally scales to terabyte datasets (see Appendix ), and the intuition can be extended for both hypothesis testing and regression for wide data (see Appendix E).

Many previous investigations have addressed similar challenges. One of the first publications on the topic composed Fisher’s LDA with PCA; the celebrated Fisherfaces paper [34]. The authors showed via a sequence of numerical experiments the utility of projecting the data using PCA prior to classifying with LDA. We extend this work by adding a supervised component to the initial projection. Moreover, we provide the geometric intuition for why and when this is advantageous, as well as show numerous examples demonstrating its superiority, as well as theoretical guarantees formalizing when LOL outperforms this approach.

Most manifold learning methods, while exhibiting both strong theoretical [35–37] and empirical performance, are fully unsupervised. Thus, in classification problems, they discover a low-dimensional representation of the data, ignoring the labels. This approach can be highly problematic when the discriminant dimensions and the directions of maximal variance in the learned manifold are not aligned (see Figure 1 for an example). Moreover, nonlinear manifold learning techniques tend to learn a mapping from the original samples to a low-dimensional space, but do not learn a projection, meaning that

new samples cannot easily be mapped onto the low-dimensional space, a requirement for supervised learning.

Another recent set of methods is collectively called “sufficient dimensionality reduction” or “first two moments” methods [38–42]. These methods are theoretically elegant, but typically require the sample size to be larger than the number of observed dimensions (although see [43] for some promising work). More recently, communication-inspired classification approaches have yielded theoretical bounds on linear and affine classification performance [44]; they do not, however, explicitly compare different projections, and the bounds we provide are more general and tighter. Other approaches formulate an optimization problem, such as projection pursuit [45], empirical risk minimization [46], or supervised dictionary learning [22]. These methods are limited because they are prone to fall into local minima, require costly iterative algorithms, and lack any theoretical guarantees on classification accuracy [46].

Other approaches, such as higher criticism thresholding [47] effectively filter the dimensions, possibly prior to performing PCA on the remaining features [48]. These approaches could be combined with LOL in ultrahigh-dimensional problems. Similarly, another recently proposed supervised PCA builds on the elegant Hilbert-Schmidt independence criterion [49] to learn an embedding [50]. Our theory demonstrates that under the Gaussian model, composing this linear projection with the difference of the means will improve subsequent performance under general settings, implying that this will be a fertile avenue to pursue.

Finally, several distributed machine learning libraries have become available, including Apache Spark’s mllib, H2O, Dato, and Vowpal Wabbit [12]. These focus almost entirely on large sample size and low-dimensionality regimes, whereas the motivating problems of interest for this work are small sample size and high-dimensionality. Moreover, they use a distributed platform that is susceptible to low bandwidth communication between nodes, meaning that as one adds resources, the computations cannot scale out optimally, as our LOL implementation does.

In conclusion, the LOL idea, appending the mean difference vector to convert unsupervised manifold learning to supervised manifold learning, has many potential applications and extensions. We have presented the first few. Incorporating additional nonlinearities via kernel methods [51], ensemble methods [52] such as random forests [53], and multiscale methods [37] are all of immediate interest. MATLAB, R, and FlashR code for the experiments performed in this manuscript are available from <http://neurodata.io/tools/LOL/>.

## A Theoretical Background

### I.A The Classification Problem

Let  $(\mathbf{X}, Y)$  be a pair of random variables, jointly sampled from  $F := F_{\mathbf{X},Y} = F_{\mathbf{X}|Y}F_Y$ . Let  $\mathbf{X}$  be a multivariate vector-valued random variable, such that its realizations live in  $p$  dimensional Euclidean space,  $\mathbf{x} \in \mathbb{R}^p$ . Let  $Y$  be a categorical random variable, whose realizations are discrete,  $y \in \{0, 1, \dots, C\}$ . The goal of a classification problem is to find a function  $g(\mathbf{x})$  such that its output tends to be the true class label  $y$ :

$$g^*(\mathbf{x}) := \operatorname{argmax}_{g \in \mathcal{G}} \mathbb{P}[g(\mathbf{x}) = y].$$

When the joint distribution of the data is known, then the Bayes optimal solution is:

$$g^*(\mathbf{x}) := \operatorname{argmax}_y f_{y,\mathbf{x}} = \operatorname{argmax}_y f_{\mathbf{x}|y}f_y = \operatorname{argmax}_y \{\log f_{\mathbf{x}|y} + \log f_y\} \quad (1)$$

Denote expected misclassification rate of classifier  $g$  for a given joint distribution  $F$ ,

$$L_g^F := \mathbb{E}[g(\mathbf{x}) \neq y] := \int \mathbb{P}[g(\mathbf{x}) \neq y] f_{\mathbf{x},y} d\mathbf{x} dy,$$

where  $\mathbb{E}$  is the expectation, which in this case, is with respect to  $F_{\mathbf{X},Y}$ . For brevity, we often simply write  $L_g$ , and we define  $L_* := L_{g^*}$ .

### I.B Linear Discriminant Analysis (LDA)

Linear Discriminant Analysis (LDA) is an approach to classification that uses a linear function of the first two moments of the distribution of the data. More specifically, let  $\boldsymbol{\mu}_j = \mathbb{E}[F_{\mathbf{X}|Y=j}]$  denote the class conditional mean, and let  $\boldsymbol{\Sigma} = \mathbb{E}[F_{\mathbf{X}}^2]$  denote the joint covariance matrix, and  $\pi_j = \mathbb{P}[Y = j]$ . Using this notation, we can define the LDA classifier:

$$g_{LDA}(\mathbf{x}) := \operatorname{argmin}_y \frac{1}{2}(\mathbf{x} - \boldsymbol{\mu}_0)^\top \boldsymbol{\Sigma}^{-1}(\mathbf{x} - \boldsymbol{\mu}_0) + \mathbb{I}\{Y = y\} \log \pi_y,$$

where  $\mathbb{I}\{\cdot\}$  is one when its argument is true, and zero otherwise. Let  $L_{LDA}^F$  be the misclassification rate of the above classifier for distribution  $F$ . Assuming equal class prior and centered means,  $\pi_0 = \pi_1$  and  $(\boldsymbol{\mu}_0 + \boldsymbol{\mu}_1)/2 = \mathbf{0}$ , re-arranging a bit, we obtain

$$g_{LDA}(\mathbf{x}) := \operatorname{argmin}_y \mathbf{x}^\top \boldsymbol{\Sigma}^{-1} \boldsymbol{\mu}_y.$$

In words, the LDA classifier chooses the class that maximizes the magnitude of the projection of an input vector  $\mathbf{x}$  onto  $\boldsymbol{\Sigma}^{-1} \boldsymbol{\mu}_y$ . When there are only two classes, letting  $\boldsymbol{\delta} = \boldsymbol{\mu}_0 - \boldsymbol{\mu}_1$ , the above further simplifies to

$$g_{2LDA}(\mathbf{x}) := \mathbb{I}\{\mathbf{x}^\top \boldsymbol{\Sigma}^{-1} \boldsymbol{\delta} > 0\}.$$

Note that the equal class prior and centered means assumptions merely changes the threshold constant from 0 to some other constant.

## I.C LDA Model

A statistical model is a family of distributions indexed by a parameter  $\theta \in \Theta$ ,  $\mathcal{F}_\theta = \{F_\theta : \theta \in \Theta\}$ . Consider the special case of the above where  $F_{\mathbf{X}|Y=y}$  is a multivariate Gaussian distribution,  $\mathcal{N}(\boldsymbol{\mu}_y, \boldsymbol{\Sigma})$ , where each class has its own mean, but all classes have the same covariance. We refer to this model as the LDA model. Let  $\theta = (\boldsymbol{\pi}, \boldsymbol{\mu}, \boldsymbol{\Sigma})$ , and let  $\Theta_{C-LDA} = (\Delta_C, \mathbb{R}^{p \times C}, \mathbb{R}_{>0}^{p \times p})$ , where  $\boldsymbol{\mu} = (\boldsymbol{\mu}_1, \dots, \boldsymbol{\mu}_C)$ ,  $\Delta_C$  is the  $C$  dimensional simplex, that is  $\Delta_C = \{\mathbf{x} : x_i \geq 0 \forall i, \sum_i x_i = 1\}$ , and  $\mathbb{R}_{>0}^{p \times p}$  is the set of positive definite  $p \times p$  matrices. Denote  $\mathcal{F}_{LDA} = \{F_\theta : \theta \in \Theta_{LDA}\}$ , dropping the superscript  $C$  for brevity where appropriate. The following lemma is well known:

**Lemma 1.**  $L_{LDA}^F = L_*^F$  for any  $F \in \mathcal{F}_{LDA}$ .

Proof. Under the LDA model, the Bayes optimal classifier is available by plugging the explicit distributions into Eq. (1).  $\square$

## B Formal Definition of LOL and Related Projection Based Classifiers

Let  $\mathbf{A} \in \mathbb{R}^{d \times p}$  be a ‘‘projection matrix’’, that is, a matrix that projects  $p$ -dimensional data into a  $d$ -dimensional subspace. The question that motivated this work is: what is the best projection matrix that we can estimate, to use to ‘‘pre-process’’ the data prior to applying LDA? Projecting the data  $\mathbf{x}$  onto a low-dimensional subspace, and then classifying via LDA in that subspace is equivalent to redefining the parameters in the low-dimensional subspace,  $\boldsymbol{\Sigma}_A = \mathbf{A}\boldsymbol{\Sigma}\mathbf{A}^\top \in \mathbb{R}^{d \times d}$  and  $\boldsymbol{\delta}_A = \mathbf{A}\boldsymbol{\delta} \in \mathbb{R}^d$ , and then using  $g_{LDA}$  in the low-dimensional space. When  $C = 2$ ,  $\pi_0 = \pi_1$ , and  $(\mu_0 + \mu_1)/2 = \mathbf{0}$ , this amounts to:

$$g_A^d(x) := \mathbb{I}\{(\mathbf{A}\mathbf{x})^\top \boldsymbol{\Sigma}_A^{-1} \boldsymbol{\delta}_A > 0\}, \text{ where } \mathbf{A} \in \mathbb{R}^{d \times p}. \quad (2)$$

Let  $L_A^d := \int \mathbb{P}[g_A(\mathbf{x}) = y] f_{\mathbf{x},y} d\mathbf{x} dy$ . Our goal therefore is to be able to choose  $A$  for a given parameter setting  $\theta = (\boldsymbol{\pi}, \boldsymbol{\delta}, \boldsymbol{\Sigma})$ , such that  $L_A$  is as small as possible (note that  $L_A$  will never be smaller than  $L_*$ ).

Formally, we seek to solve the following optimization problem:

$$\begin{aligned} & \underset{\mathbf{A}}{\text{minimize}} && \mathbb{E}[\mathbb{I}\{\mathbf{x}^\top \mathbf{A}^\top \boldsymbol{\Sigma}_A^{-1} \boldsymbol{\delta}_A > 0\} \neq y] \\ & \text{subject to} && \mathbf{A} \in \mathbb{R}^{p \times d}. \end{aligned} \quad (3)$$

Let  $\mathcal{A}^d = \{\mathbf{A} : \mathbf{A} \in \mathbb{R}^{d \times p}\}$ , and let  $\mathcal{A}_* \subset \mathcal{A}$  be the set of  $\mathbf{A}$  that minimizes Eq. (3), and let  $\mathbf{A}_* \in \mathcal{A}_*$  (where we dropped the superscript  $d$  for brevity). Let  $L_{\mathbf{A}_*}^* = L_{\mathbf{A}_*}$  be the misclassification rate for any  $\mathbf{A} \in \mathcal{A}_*$ , that is,  $L_{\mathbf{A}_*}^*$  is the Bayes optimal misclassification rate for the classifier that composes  $\mathbf{A}$  with LDA.

In our opinion, Eq. (3) is the simplest supervised manifold learning problem there is: a two-class classification problem, where the data are multivariate Gaussians with shared covariances, the manifold is linear, and the classification is done via LDA. Nonetheless, solving Eq. (3) is difficult, because we do not know how to evaluate the integral analytically, and we do not know any algorithms that are guaranteed to find the global optimum in finite time. We proceed by studying a few natural choices for  $\mathbf{A}$ .

## II.A Bayes Optimal Projection

**Lemma 2.**  $\delta^\top \Sigma^{-1} \in \mathcal{A}_*$

Proof. Let  $\mathbf{B} = (\Sigma^{-1} \delta)^\top = \delta^\top (\Sigma^{-1})^\top = \delta^\top \Sigma^{-1}$ , so that  $\mathbf{B}^\top = \Sigma^{-1} \delta$ , and plugging this in to Eq. (2), we obtain

$$\begin{aligned} g_B(x) &= \mathbb{I}\{\mathbf{x}^\top \mathbf{B}^\top \Sigma_B^{-1} \delta_B > 0\} \\ &= \mathbb{I}\{\mathbf{x}^\top (\Sigma^{-1} \delta) (\Sigma_B^{-1} \delta_B) > 0\} && \text{plugging in } \mathbf{B} \\ &= \mathbb{I}\{\mathbf{x}^\top \Sigma^{-1} \delta > 0\} && \text{because } \Sigma_B^{-1} \delta_B > 0. \end{aligned}$$

In other words, letting  $\mathbf{B}$  be the Bayes optimal projection recovers the Bayes classifier, as it should. Or, more formally, for any  $F \in \mathcal{F}_{LDA}$ ,  $L_{\delta^\top \Sigma^{-1}} = L_*$   $\square$

## II.B Principle Components Analysis (PCA) Projection

Principle Components Analysis (PCA) finds the directions of maximal variance in a dataset. PCA is closely related to eigendecompositions and singular value decompositions (SVD). In particular, the top left singular vector of a matrix  $\mathbf{X} \in \mathbb{R}^{p \times n}$ , whose columns are centered, is the eigenvector with the largest eigenvalue of the centered covariance matrix  $\mathbf{X} \mathbf{X}^\top$ . SVD enables one to estimate this eigenvector without ever forming the outer product matrix, because SVD factorizes a matrix  $\mathbf{X}$  into  $\mathbf{U} \mathbf{S} \mathbf{V}^\top$ , where  $\mathbf{U}$  and  $\mathbf{V}$  are orthonormal  $p \times n$  matrices, and  $\mathbf{S}$  is a diagonal matrix, whose diagonal values are decreasing,  $s_1 \geq s_2 \geq \dots > s_n$ . Defining  $\mathbf{U} = [\mathbf{u}_1, \mathbf{u}_2, \dots, \mathbf{u}_n]$ , where each  $\mathbf{u}_i \in \mathbb{R}^p$ , then  $\mathbf{u}_i$  is the  $i^{\text{th}}$  eigenvector, and  $s_i$  is the square root of the  $i^{\text{th}}$  eigenvalue of  $\mathbf{X} \mathbf{X}^\top$ . Let  $\mathbf{A}_d^{PCA} = [\mathbf{u}_1, \dots, \mathbf{u}_d]$  be the truncated PCA orthonormal matrix, and let  $\mathbf{I}_{d \times p}$  denote a  $d \times p$  dimensional identity matrix.

The PCA matrix is perhaps the most obvious choice of an orthonormal matrix for several reasons. First, truncated PCA minimizes the squared error loss between the original data matrix and all possible rank  $d$  representations:

$$\operatorname{argmin}_{\mathbf{A} \in \mathbb{R}^{d \times p}: \mathbf{A} \mathbf{A}^\top = \mathbf{I}_{d \times d}} \|\mathbf{X} - \mathbf{A}^\top \mathbf{A}\|_F^2.$$

Second, the ubiquity of PCA has led to a large number of highly optimized numerical libraries for computing PCA (for example, LAPACK [54]).

In this supervised setting, we consider two different variants of PCA, each based on centering the data differently. For the first one, which we refer to as “pooled PCA” (or just PCA for brevity), we center the data by subtracting the “pooled mean” from each sample, that is, we let  $\tilde{\mathbf{x}}_i = \mathbf{x} - \boldsymbol{\mu}$ , where  $\boldsymbol{\mu} = \mathbb{E}[\mathbf{x}]$ . For the second, which we refer to as “class conditional PCA” (or LDA for brevity), we center the data by subtracting the “class-conditional mean” from each sample, that is, we let  $\tilde{\mathbf{x}}_i = \mathbf{x} - \boldsymbol{\mu}_y$ , where  $\boldsymbol{\mu}_y = \mathbb{E}[\mathbf{x} | Y = y]$ .

Notationally, let  $\mathbf{U}_d = [\mathbf{u}_1, \dots, \mathbf{u}_d] \in \mathbb{R}^{p \times d}$ , and note that  $\mathbf{U}_d^\top \mathbf{U}_d = \mathbf{I}_{d \times d}$  and  $\mathbf{U}_d \mathbf{U}_d^\top = \mathbf{I}_{p \times p}$ . Similarly, let  $\mathbf{U} \mathbf{S} \mathbf{U}^\top = \boldsymbol{\Sigma}$ , and  $\mathbf{U} \mathbf{S}^{-1} \mathbf{U}^\top = \boldsymbol{\Sigma}^{-1}$ . Let  $\mathbf{S}_d$  be the matrix whose diagonal entries are the eigenvalues, up to the  $d^{\text{th}}$  one, that is  $\mathbf{S}_d(i, j) = s_i$  for  $i = j \leq d$  and zero otherwise. Similarly,  $\boldsymbol{\Sigma}_d = \mathbf{U} \mathbf{S}_d \mathbf{U}^\top = \mathbf{U}_d \mathbf{S}_d \mathbf{U}_d^\top$ . Reduced-rank LDA (RR-LDA) is a regularized LDA algorithm. Specifically, rather than using the full rank covariance matrix, it uses a rank- $d$  approximation. Formally, let  $g_{LDA}^d := \mathbb{I}\{\mathbf{x}^\top \boldsymbol{\Sigma}^{-1} \delta > 0\}$  be the LDA classifier, and let  $g_{LDA}^d := \mathbb{I}\{\mathbf{x}^\top \boldsymbol{\Sigma}_d^{-1} \delta > 0\}$  be the regularized

LDA classifier, that is, the LDA classifier where the the bottom  $p - d$  eigenvalues of the covariance matrix are set to zero.

**Lemma 3.** Using LDA to pre-process the data, then using LDA on the projected data, is equivalent to RR-LDA. More succinctly,  $L_{LDA \circ LDA}^d = L_{RR-LDA}^d$ .

Proof. Plugging  $\mathbf{U}_d$  into Eq. (2) for  $\mathbf{A}$ , and considering only the left side of the operand, we have

$$\begin{aligned}
(\mathbf{Ax})^\top \Sigma_A^{-1} \delta_A &= \mathbf{x}^\top \mathbf{A}^\top \mathbf{A} \Sigma^{-1} \mathbf{A}^\top \mathbf{A} \delta, \\
&= \mathbf{x}^\top \mathbf{U}_d \mathbf{U}_d^\top \Sigma^{-1} \mathbf{U}_d \mathbf{U}_d^\top \delta, \\
&= \mathbf{x}^\top \mathbf{U}_d \mathbf{U}_d^\top \mathbf{U} \mathbf{S}^{-1} \mathbf{U}^\top \mathbf{U}_d \mathbf{U}_d^\top \delta, \\
&= \mathbf{x}^\top \mathbf{U}_d \mathbf{I}_{d \times p} \mathbf{S}^{-1} \mathbf{I}_{p \times d} \mathbf{U}_d^\top \delta, \\
&= \mathbf{x}^\top \mathbf{U}_d \mathbf{S}_d^{-1} \mathbf{U}_d^\top \delta, \\
&= \mathbf{x}^\top \Sigma_d^{-1} \delta
\end{aligned}$$

as desired. □

The implication of this lemma is that if one desires to implement RR-LDA, rather than first learning the eigenvectors and then learning LDA, one can instead directly implement regularized LDA by setting the bottom  $p - d$  eigenvalues to zero. This latter approach removes the requirement to run SVD twice, therefore reducing the computational burden as well as the possibility of numerical instability issues.

## II.C Linear Optimal Low-Rank (LOL) Projection

The basic idea of LOL is to use both  $\delta$  and the top  $d$  eigenvectors of the class-conditionally centered covariance. When there are only two classes,  $\delta = \mu_0 - \mu_1$ . When there are  $C > 2$  classes, there are  $\binom{C}{2} = \frac{C!}{2(C-2)!}$  pairwise combinations,  $\delta_{ij} = \mu_i - \mu_j$  for all  $i \neq j$ . However, since  $\binom{C}{2}$  is nearly  $C^2$ , when  $C$  is large, this would mean incorporating many mean difference vectors. Note that  $[\delta_{1,2}, \delta_{1,3}, \dots, \delta_{C-1,C}]$  is in fact a rank  $C - 1$  matrix, because it is a linear function of the  $C$  different means. Therefore, we only need  $C - 1$  differences to span the space of all pairwise differences. To mitigate numerical instability issues, we adopt the following convention. For each class, estimate the expected mean and the number of samples per class,  $\mu_c$  and  $\pi_c$ . Sort the means in order of decreasing  $\pi_c$ , so that  $\pi_{(1)} > \pi_{(2)} > \dots > \pi_{(C)}$ . Then, subtract  $\mu_{(1)}$  from all other means:  $\delta_i = \mu_{(1)} - \mu_{(i)}$ , for  $i = 2, \dots, C$ . Finally,  $\delta = [\delta_1, \dots, \delta_C]$ .

Given  $\delta$  and  $\mathbf{A}_{LDA}^{d-1}$ , to obtain LOL naïvely, we could simply concatenate the two,  $\mathbf{A}_{LOL}^d = [\delta, \mathbf{A}_{LDA}^{d-1}]$ . Recall that eigenvectors are orthonormal. To maintain orthonormality between the eigenvectors and vectors of  $\delta$ , we could easily apply Gram-Schmidt,  $\mathbf{A}_{LOL}^d = \text{Orth}([\delta, \mathbf{A}_{LDA}^{d-1}])$ . In practice, this orthogonalization step does not matter much, so we ignore it hereafter. To ensure that  $\delta$  and  $\Sigma$  are balanced appropriately, we normalize each vector in  $\delta$  to have norm unity. Formally, let  $\tilde{\delta}_j = \delta_j / \|\delta_j\|$ , where  $\delta_j$  is the  $j^{\text{th}}$  difference of the mean vector and let  $\mathbf{A}_{LOL}^d = [\tilde{\delta}, \mathbf{A}_{LDA}^{d-(C-1)}]$ .

When the distribution of the data is not provided, each of the above terms must be estimated from the

data. We use the maximum likelihood estimators for each, specifically:

$$\hat{\pi}_c = \frac{1}{n} \sum_{i=1}^n \mathbb{I}\{y_i = c\}, \quad (4)$$

$$\hat{\boldsymbol{\mu}} = \frac{1}{n} \sum_{i=1}^n \mathbf{x}_i, \quad (5)$$

$$\hat{\boldsymbol{\mu}}_c = \frac{1}{n} \sum_{i=1}^n \mathbf{x}_i \mathbb{I}\{y_i = c\}. \quad (6)$$

For completeness, below we provide pseudocode for learning the sample version of LOL. The population version does not require the estimation of the parameters, as the known parameters can simply be used.

## II.D LDA is rotationally invariant

For certain classification tasks, the observed dimensions (or features) have intrinsic value, e.g. when simple interpretability is desired. However, in many other contexts, interpretability is less important [55]. When the exploitation task at hand is invariant to rotations, then we have no reason to restrict our search space to be sparse in the observed dimensions. For example, we can consider sparsity in the eigenvector basis. Fisherfaces is one example of a rotationally invariant classifier, under certain model assumptions. Let  $\mathbf{W}$  be a rotation matrix, that is  $\mathbf{W} \in \mathcal{W} = \{\mathbf{W} : \mathbf{W}^\top = \mathbf{W}^{-1} \text{ and } \det(\mathbf{W}) = 1\}$ . Moreover, let  $\mathbf{W} \circ F$  denote the distribution  $F$  after transformation by an operator  $\mathbf{W}$ . For example, if  $F = \mathcal{N}(\boldsymbol{\mu}, \boldsymbol{\Sigma})$  then  $\mathbf{W} \circ F = \mathcal{N}(\mathbf{W}\boldsymbol{\mu}, \mathbf{W}\boldsymbol{\Sigma}\mathbf{W}^\top)$ .

**Definition 1.** A rotationally invariant classifier has the following property:

$$L_g^F = L_g^{\mathbf{W} \circ F}, \quad F \in \mathcal{F} \text{ and } \mathbf{W} \in \mathcal{W}.$$

In words, the Bayes risk of using classifier  $g$  on distribution  $F$  is unchanged if  $F$  is first rotated.

Now, we can state the main lemma of this subsection: LDA is rotationally invariant.

**Lemma 4.**  $L_{LDA}^F = L_{LDA}^{\mathbf{W} \circ F}$ , for any  $F \in \mathcal{F}$ .

Proof. LDA is in fact simply thresholding  $\mathbf{x}^\top \boldsymbol{\Sigma}^{-1} \boldsymbol{\delta}$  whenever its value is larger than some constant. Thus, we can demonstrate rotational invariance by demonstrating that  $\mathbf{x}^\top \boldsymbol{\Sigma}^{-1} \boldsymbol{\delta}$  is rotationally invariant.

$$\begin{aligned} (\mathbf{W}\mathbf{x})^\top (\mathbf{W}\boldsymbol{\Sigma}\mathbf{W}^\top)^{-1} \mathbf{W}\boldsymbol{\delta} &= \mathbf{x}^\top \mathbf{W}^\top (\mathbf{W}\mathbf{U}\mathbf{S}\mathbf{U}^\top \mathbf{W}^\top)^{-1} \mathbf{W}\boldsymbol{\delta} && \text{by substituting } \mathbf{U}\mathbf{S}\mathbf{U}^\top \text{ for } \boldsymbol{\Sigma} \\ &= \mathbf{x}^\top \mathbf{W}^\top (\tilde{\mathbf{U}}\tilde{\mathbf{S}}\tilde{\mathbf{U}}^\top)^{-1} \mathbf{W}\boldsymbol{\delta} && \text{by letting } \tilde{\mathbf{U}} = \mathbf{W}\mathbf{U} \\ &= \mathbf{x}^\top \mathbf{W}^\top (\tilde{\mathbf{U}}\tilde{\mathbf{S}}^{-1}\tilde{\mathbf{U}}^\top) \mathbf{W}\boldsymbol{\delta} && \text{by the laws of matrix inverse} \\ &= \mathbf{x}^\top \mathbf{W}^\top \mathbf{W}\mathbf{U}\tilde{\mathbf{S}}^{-1}\mathbf{U}^\top \mathbf{W}^\top \mathbf{W}\boldsymbol{\delta} && \text{by un-substituting } \mathbf{W}\mathbf{U} = \tilde{\mathbf{U}} \\ &= \mathbf{x}^\top \mathbf{U}\tilde{\mathbf{S}}^{-1}\mathbf{U}^\top \boldsymbol{\delta} && \text{because } \mathbf{W}^\top \mathbf{W} = \mathbf{I} \\ &= \mathbf{x}^\top \boldsymbol{\Sigma}^{-1} \boldsymbol{\delta} && \text{by un-substituting } \mathbf{U}\tilde{\mathbf{S}}^{-1}\mathbf{U}^\top = \boldsymbol{\Sigma} \end{aligned}$$

□

One implication of this lemma is that we can reparameterize without loss of generality. Specifically, defining  $\mathbf{W} := \mathbf{U}^\top$  yields a change of variables:  $\Sigma \mapsto \mathbf{S}$  and  $\delta \mapsto \mathbf{U}^\top \delta := \delta''$ , where  $\mathbf{S}$  is a diagonal covariance matrix. Moreover, let  $\mathbf{d} = (\sigma_1, \dots, \sigma_D)^\top$  be the vector of eigenvalues, then  $\mathbf{S}^{-1} \delta' = \mathbf{d}^{-1} \odot \tilde{\delta}$ , where  $\odot$  is the Hadamard (entrywise) product. The LDA classifier may therefore be encoded by a unit vector,  $\tilde{\mathbf{d}} := \frac{1}{m} \mathbf{d}^{-1} \odot \tilde{\delta}'$ , and its magnitude,  $m := \|\mathbf{d}^{-1} \odot \tilde{\delta}\|$ . This will be useful later.

## II.E Rotation of Projection Based Linear Classifiers $g_A$

By a similar argument as above, one can easily show that:

$$\begin{aligned} (\mathbf{A}\mathbf{W}\mathbf{x})^\top (\mathbf{A}\mathbf{W}\Sigma\mathbf{W}^\top \mathbf{A}^\top)^{-1} \mathbf{A}\mathbf{W}\delta &= \mathbf{x}^\top (\mathbf{W}^\top \mathbf{A}^\top) (\mathbf{A}\mathbf{W}) \Sigma^{-1} (\mathbf{W}^\top \mathbf{A}^\top) (\mathbf{A}\mathbf{W}) \delta \\ &= \mathbf{x}^\top \mathbf{Y}^\top \mathbf{Y} \Sigma^{-1} \mathbf{Y}^\top \mathbf{Y} \delta \\ &= \mathbf{x}^\top \mathbf{Z} \Sigma^{-1} \mathbf{Z}^\top \delta \\ &= \mathbf{x}^\top (\mathbf{Z} \Sigma \mathbf{Z}^\top)^{-1} \delta = \mathbf{x}^\top \tilde{\Sigma}_d^{-1} \delta, \end{aligned}$$

where  $\mathbf{Y} = \mathbf{A}\mathbf{W} \in \mathbb{R}^{d \times p}$  so that  $\mathbf{Z} = \mathbf{Y}^\top \mathbf{Y}$  is a symmetric  $p \times p$  matrix of rank  $d$ . In other words, rotating and then projecting is equivalent to a change of basis. The implications of the above is:

**Lemma 5.**  $g_A$  is rotationally invariant if and only if  $\text{span}(\mathbf{A}) = \text{span}(\Sigma_d)$ . In other words, LDA is the only rotationally invariant projection.

## C Simulations

Let  $f_{x|y}$  denote the conditional distribution of  $X$  given  $Y$ , and let  $f_y$  denote the prior probability of  $Y$ . For simplicity, assume that realizations of the random variable  $X$  are  $p$ -dimensional vectors,  $x \in \mathbb{R}^p$ , and realizations of the random variable  $Y$  are binary,  $y \in \{0, 1\}$ . For most simulation settings, each class is Gaussian:  $f_{x|y} = \mathcal{N}(\mu_y, \Sigma_y)$ , where  $\mu_y$  is the class-conditional mean and  $\Sigma_y$  is the class-conditional covariance. Moreover, we assume  $f_y$  is a Bernoulli distribution with probability  $\pi$  that  $y = 1$ ,  $f_y = \mathcal{B}(\pi)$ . We typically assume that both classes are equally likely,  $\pi = 0.5$ , and the covariance matrices are the same,  $\Sigma_0 = \Sigma_1 = \Sigma$ . Under such assumptions, we merely specify  $\theta = \{\mu_0, \mu_1, \Sigma\}$ . We consider the following simulation settings:

### Stacked Cigars

- $\mu_0 = \mathbf{0}$ ,
- $\mu_1 = (a, b, a, \dots, a)$ ,
- $\Sigma$  is a diagonal matrix, with diagonal vector,  $\mathbf{d} = (1, b, 1, \dots, 1)$ ,

where  $a = 0.15$  and  $b = 4$ .

### Trunk

- $\mu_0 = b / \sqrt{(1, 3, 5, \dots, 2p)}$ ,
- $\mu_1 = -\mu_0$ ,
- $\Sigma$  is a diagonal matrix, with diagonal vector,  $\mathbf{d} = 100 / \sqrt{(p, p-1, p-2, \dots, 1)}$ ,

where  $b = 4$ .

### Rotated Trunk

Same as Trunk, but the data are randomly rotated, that is, we sample  $Q$  uniformly from the set of  $p$ -dimensional rotation matrices, and then set:

- $\mu_0 \leftarrow Q\mu_0$ ,
- $\mu_1 \leftarrow Q\mu_1$ ,
- $\Sigma \leftarrow Q\Sigma Q^T$ .

### Toeplitz

- $\mu_0 = b \times (1, -1, 1, -1, \dots, 1)$ ,
- $\mu_1 = -\mu_0$ ,
- $\Sigma$  is a Toeplitz matrix, where the top row is  $\rho^{(0,1,2,\dots,p-1)}$ ,

where  $b$  is a function of the Toeplitz matrix such that the noise stays constant as dimensionality increases, and  $\rho = 0.5$ .

### 3 Classes

Same as Trunk, but with a third mean equal to the zero vector,  $\mu_2 = \mathbf{0}$ .

### Fat Tails

For this setting, each class is actually a mixture of two Gaussians with the same mean (the two classes have the same covariances):

- $\mu_0 = \mathbf{0}$ ,
- $\mu_1 = (0, \dots, 0, 1, \dots, 1)$ , where the first  $s = 10$  elements are zero,
- $\Sigma_0$  is a matrix with 1's on the diagonal, and 0.2 on the off diagonal,
- $\Sigma_1 = 15 \times \Sigma_0$ ,

and then we randomly rotated as in the rotated Trunk example.

### QDA

A generalization of the Toeplitz setting, where the two classes have two different covariance matrices, meaning that the optimal discriminant boundary is quadratic.

- $\mu_0 = b \times (1, -1, 1, -1, \dots, 1)$ ,
- $\mu_1 = -Q \times (\mu_0 + 0.1)$ ,
- $\Sigma_0$  is the same Toeplitz matrix as described above, and
- $\Sigma_1 = Q\Sigma_0Q^T$ .

### Computational Efficiency Experiments

These experiments used the Trunk setting, increasing the observed dimensionality.

### Hypothesis Testing Experiments

We considered two related joint distributions here. The first joint (Diagonal) is described by:

- $\mu_0 = \mathbf{0}$ ,

- $\tilde{\boldsymbol{\mu}}_1 \sim \mathcal{N}(\mathbf{0}, \mathbf{I})$ ,  $\boldsymbol{\mu}_1 = \tilde{\boldsymbol{\mu}}_1 / \|\tilde{\boldsymbol{\mu}}_1\|$ ,
- $\boldsymbol{\Sigma}$  is the same Toeplitz matrix as described above, rescaled to have a Frobenius norm of 50.

The second (Dense) is the same except that the eigenvectors are uniformly random sampled orthonormal matrices, rather than the identity matrix.

## Regression Experiments

In this experiment we used a distribution similar to the Toeplitz distribution as described above, but  $y$  was a linear function of  $x$ , that is,  $y = Ax$ , where  $x \sim \mathcal{N}(\mathbf{0}, \boldsymbol{\Sigma})$ , where  $\boldsymbol{\Sigma}$  is the above described Toeplitz matrix, and  $A$  is a diagonal matrix whose first two diagonal elements are non-zero, and the rest are zero.

# D Theorems and Proofs of Main Result

## IV.A Chernoff information

We now introduce the notion of the Chernoff information, which serves as our surrogate measure for the Bayes error of any classification procedure given the projected data – in the context of this paper the projection is via LOL or PCA. Our discussion of the Chernoff information is under the context of decision rules for hypothesis testing, nevertheless, as evidenced by the fact that the maximum a posteriori decision rule—equivalently the Bayes classifier—achieves the Chernoff information rate, this distinction between hypothesis testing and classification is mainly for ease of exposition.

Let  $F_0$  and  $F_1$  be two absolutely continuous multivariate distributions in  $\Omega \subset \mathbb{R}^d$  with density functions  $f_0$  and  $f_1$ , respectively. Suppose that  $X_1, X_2, \dots, X_m$  are independent and identically distributed random variables, with  $X_i$  distributed either  $F_0$  or  $F_1$ . We are interested in testing the simple null hypothesis  $\mathbb{H}_0: F = F_0$  against the simple alternative hypothesis  $\mathbb{H}_1: F = F_1$ . A test  $T$  is a sequence of mapping  $T_m: \Omega^m \mapsto \{0, 1\}$  such that given  $X_1 = x_1, X_2 = x_2, \dots, X_m = x_m$ , the test rejects  $\mathbb{H}_0$  in favor of  $\mathbb{H}_1$  if  $T_m(x_1, x_2, \dots, x_m) = 1$ ; similarly, the test decides  $\mathbb{H}_1$  instead of  $\mathbb{H}_0$  if  $T_m(x_1, x_2, \dots, x_m) = 0$ . The Neyman-Pearson lemma states that, given  $X_1 = x_1, X_2 = x_2, \dots, X_m = x_m$  and a threshold  $\eta_m \in \mathbb{R}$ , the likelihood ratio test rejects  $\mathbb{H}_0$  in favor of  $\mathbb{H}_1$  whenever

$$\left( \sum_{i=1}^m \log f_0(x_i) - \sum_{i=1}^m \log f_1(x_i) \right) \leq \eta_m.$$

Moreover, the likelihood ratio test is the most powerful test at significance level  $\alpha_m = \alpha(\eta_m)$ , i.e., the likelihood ratio test minimizes the type II error  $\beta_m$  subject to the constraint that the type I error is at most  $\alpha_m$ .

Assume that  $\pi \in (0, 1)$  is a prior probability of  $\mathbb{H}_0$  being true. Then, for a given  $\alpha_m^* \in (0, 1)$ , let  $\beta_m^* = \beta_m^*(\alpha_m^*)$  be the type II error associated with the likelihood ratio test when the type I error is at most  $\alpha_m^*$ . The quantity  $\inf_{\alpha_m^* \in (0, 1)} \pi \alpha_m^* + (1 - \pi) \beta_m^*$  is then the Bayes risk in deciding between  $\mathbb{H}_0$  and  $\mathbb{H}_1$  given the  $m$  independent random variables  $X_1, X_2, \dots, X_m$ . A classical result of Chernoff [18] states that the Bayes risk is intrinsically linked to a quantity known as the Chernoff information. More

specifically, let  $C(F_0, F_1)$  be the quantity

$$\begin{aligned} C(F_0, F_1) &= -\log \left[ \inf_{t \in (0,1)} \int_{\mathbb{R}^d} f_0^t(\mathbf{x}) f_1^{1-t}(\mathbf{x}) d\mathbf{x} \right] \\ &= \sup_{t \in (0,1)} \left[ -\log \int_{\mathbb{R}^d} f_0^t(\mathbf{x}) f_1^{1-t}(\mathbf{x}) d\mathbf{x} \right] \end{aligned} \quad (7)$$

Then we have

$$\lim_{m \rightarrow \infty} \frac{1}{m} \inf_{\alpha_m^* \in (0,1)} \log(\pi \alpha_m^* + (1-\pi) \beta_m^*) = -C(F_0, F_1). \quad (8)$$

Thus  $C(F_0, F_1)$  is the exponential rate at which the Bayes error  $\inf_{\alpha_m^* \in (0,1)} \pi \alpha_m^* + (1-\pi) \beta_m^*$  decreases as  $m \rightarrow \infty$ ; we also note that the  $C(F_0, F_1)$  is independent of  $\pi$ . We also define, for a given  $t \in (0, 1)$  the Chernoff divergence  $C_t(F_0, F_1)$  between  $F_0$  and  $F_1$  by

$$C_t(F_0, F_1) = -\log \int_{\mathbb{R}^d} f_0^t(\mathbf{x}) f_1^{1-t}(\mathbf{x}) d\mathbf{x}.$$

The Chernoff divergence is an example of a  $f$ -divergence as defined in [56]. When  $t = 1/2$ ,  $C_t(F_0, F_1)$  is the Bhattacharyya distance between  $F_0$  and  $F_1$ .

The result of Eq. (8) can be extended to  $K+1 \geq 2$  hypothesis, with the exponential rate being the minimum of the Chernoff information between any pair of hypothesis. More specifically, let  $F_0, F_1, \dots, F_K$  be distributions on  $\mathbb{R}^d$  and let  $X_1, X_2, \dots, X_m$  be independent and identically distributed random variables with distribution  $F \in \{F_0, F_1, \dots, F_K\}$ . Our inference task is in determining the distribution of the  $X_i$  among the  $K+1$  hypothesis  $\mathbb{H}_0: F = F_0, \dots, \mathbb{H}_K: F = F_K$ . Suppose also that hypothesis  $\mathbb{H}_k$  has a priori probability  $\pi_k$ . For any decision rule  $g$ , the risk of  $g$  is  $r(g) = \sum_k \pi_k \sum_{l \neq k} \alpha_{lk}(g)$  where  $\alpha_{lk}(g)$  is the probability of accepting hypothesis  $\mathbb{H}_l$  when hypothesis  $\mathbb{H}_k$  is true. Then we have [57]

$$\inf_g \lim_{m \rightarrow \infty} \frac{r(g)}{m} = -\min_{k \neq l} C(F_k, F_l), \quad (9)$$

where the infimum is over all decision rules  $g$ , i.e., for any  $g$ ,  $r(g)$  decreases to 0 as  $m \rightarrow \infty$  at a rate no faster than  $\exp(-m \min_{k \neq l} C(F_k, F_l))$ .

When the distributions  $F_0$  and  $F_1$  are multivariate normal, that is,  $F_0 = \mathcal{N}(\mu_0, \Sigma_0)$  and  $F_1 = \mathcal{N}(\mu_1, \Sigma_1)$ ; then, denoting by  $\Sigma_t = t\Sigma_0 + (1-t)\Sigma_1$ , we have

$$C(F_0, F_1) = \sup_{t \in (0,1)} \left( \frac{t(1-t)}{2} (\mu_1 - \mu_2)^\top \Sigma_t^{-1} (\mu_1 - \mu_2) + \frac{1}{2} \log \frac{|\Sigma_t|}{|\Sigma_0|^t |\Sigma_1|^{1-t}} \right).$$

## IV.B Projecting data and Chernoff information

We now discuss how the Chernoff information characterizes the effect a linear transformation  $A$  of the data has on classification accuracy. We start with the following simple result whose proof follows directly from Eq. (9).

**Lemma 6.** Let  $F_0 = \mathcal{N}(\mu_0, \Sigma)$  and  $F_1 \sim \mathcal{N}(\mu_1, \Sigma)$  be two multivariate normals with equal covariance matrices. For any linear transformation  $A$ , let  $F_0^{(A)}$  and  $F_1^{(A)}$  denote the distribution of  $AX$  when

$X \sim F_0$  and  $X \sim F_1$ , respectively. We then have

$$\begin{aligned} C(F_0^{(A)}, F_1^{(A)}) &= \frac{1}{8}(\mu_1 - \mu_0)^\top A^\top (A\Sigma A^\top)^{-1} A(\mu_1 - \mu_0) \\ &= \frac{1}{8}(\mu_1 - \mu_0)^\top \Sigma^{-1/2} \Sigma^{1/2} A^\top (A\Sigma A^\top)^{-1} A \Sigma^{1/2} \Sigma^{-1/2} (\mu_1 - \mu_0) \\ &= \frac{1}{8} \|P_{\Sigma^{1/2} A^\top} \Sigma^{-1/2} (\mu_1 - \mu_0)\|_F^2 \end{aligned} \quad (10)$$

where  $P_Z = Z(Z^\top Z)^{-1} Z^\top$  denotes the matrix corresponding to the orthogonal projection onto the columns of  $Z$ .

Thus for a classification problem where  $X|Y=0$  and  $X|Y=1$  are distributed multivariate normals with mean  $\mu_0$  and  $\mu_1$  and the same covariance matrix  $\Sigma$ , Lemma 6 then states that for any two linear transformations  $A$  and  $B$ , the transformed data  $AX$  is to be preferred over the transformed data  $BX$  if

$$(\mu_1 - \mu_0)^\top A^\top (A\Sigma A^\top)^{-1} A(\mu_1 - \mu_0) > (\mu_1 - \mu_0)^\top B^\top (B\Sigma B^\top)^{-1} B(\mu_1 - \mu_0).$$

In particular, using Lemma 6, we obtain the following result showing the dominance of LOL over PCA' when the class conditional distributions are multivariate normal with a common variance.

**Theorem 1.** Let  $F_0 = N(\mu_0, \Sigma)$  and  $F_1 \sim N(\mu_1, \Sigma)$  be multivariate normal distributions in  $\mathbb{R}^p$ . Let  $\lambda_1 \geq \lambda_2 \geq \dots \geq \lambda_p$  be the eigenvalues of  $\Sigma$  and  $u_1, u_2, \dots, u_p$  the corresponding eigenvectors. For  $d \leq p$ , let  $U_d = [u_1 | u_2 | \dots | u_d] \in \mathbb{R}^{p \times d}$  be the matrix whose columns are the eigenvectors  $u_1, u_2, \dots, u_d$ . Let  $A = [\delta | U_{d-1}]$  and  $B = U_d$  be the LOL and PCA' linear transformations into  $\mathbb{R}^d$ , respectively. Then

$$\begin{aligned} C(F_0^{(A)}, F_1^{(A)}) - C(F_0^{(B)}, F_1^{(B)}) &= \frac{(\delta^\top (I - U_{d-1} U_{d-1}^\top) \delta)^2}{\delta^\top (\Sigma - \Sigma_{d-1}) \delta} - \delta^\top (\Sigma_d^\dagger - \Sigma_{d-1}^\dagger) \delta \\ &\geq \frac{1}{\lambda_d} \delta^\top (I - U_{d-1} U_{d-1}^\top) \delta - \frac{1}{\lambda_d} \delta^\top (U_d U_d^\top - U_{d-1} U_{d-1}^\top) \delta \geq 0 \end{aligned} \quad (11)$$

and the inequality is strict whenever  $\delta^\top (I - U_d U_d^\top) \delta > 0$ .

Proof. We first note that

$$A\Sigma A^\top = [\delta | U_{d-1}]^\top \Sigma [\delta | U_{d-1}] = \begin{bmatrix} \delta^\top \Sigma \delta & \delta^\top \Sigma U_{d-1} \\ U_{d-1}^\top \Sigma \delta & U_{d-1}^\top \Sigma U_{d-1} \end{bmatrix} = \begin{bmatrix} \delta^\top \Sigma \delta & \delta^\top \Sigma U_{d-1} \\ U_{d-1}^\top \Sigma \delta & \Lambda_{d-1} \end{bmatrix}$$

where  $\Lambda_{d-1} = \text{diag}(\lambda_1, \lambda_2, \dots, \lambda_{d-1})$  is the  $(d-1) \times (d-1)$  diagonal matrix formed by the eigenvalues  $\lambda_1, \lambda_2, \dots, \lambda_{d-1}$ . Therefore, letting  $\gamma = \delta^\top \Sigma \delta - \delta^\top \Sigma U_{d-1} \Lambda_{d-1}^{-1} U_{d-1}^\top \Sigma \delta$ , we have

$$\begin{aligned} (A\Sigma A^\top)^{-1} &= \begin{bmatrix} \delta^\top \Sigma \delta & \delta^\top \Sigma U_{d-1} \\ U_{d-1}^\top \Sigma \delta & U_{d-1}^\top \Sigma U_{d-1} \end{bmatrix}^{-1} \\ &= \begin{bmatrix} \gamma^{-1} & -\delta^\top \Sigma U_{d-1} \Lambda_{d-1}^{-1} \gamma^{-1} \\ -\Lambda_{d-1}^{-1} U_{d-1}^\top \Sigma \delta \gamma^{-1} & (\Lambda_{d-1} - \frac{U_{d-1}^\top \Sigma \delta \delta^\top \Sigma U_{d-1}}{\delta^\top \Sigma \delta})^{-1} \end{bmatrix}. \end{aligned}$$

The Sherman-Morrison-Woodbury formula then implies

$$\begin{aligned} \left( \Lambda_{d-1} - \frac{U_{d-1}^\top \Sigma \delta \delta^\top \Sigma U_{d-1}}{\delta^\top \Sigma \delta} \right)^{-1} &= \Lambda_{d-1}^{-1} + \frac{\Lambda_{d-1}^{-1} U_{d-1}^\top \Sigma \delta \delta^\top \Sigma U_{d-1} \Lambda_{d-1}^{-1} / (\delta^\top \Sigma \delta)}{1 - \delta^\top \Sigma U_{d-1} \Lambda_{d-1}^{-1} U_{d-1}^\top \Sigma \delta / (\delta^\top \Sigma \delta)} \\ &= \Lambda_{d-1}^{-1} + \frac{\Lambda_{d-1}^{-1} U_{d-1}^\top \Sigma \delta \delta^\top \Sigma U_{d-1} \Lambda_{d-1}^{-1}}{\delta^\top \Sigma \delta - \delta^\top \Sigma U_{d-1} \Lambda_{d-1}^{-1} U_{d-1}^\top \Sigma \delta} \\ &= \Lambda_{d-1}^{-1} + \gamma^{-1} \Lambda_{d-1}^{-1} U_{d-1}^\top \Sigma \delta \delta^\top \Sigma U_{d-1} \Lambda_{d-1}^{-1} \end{aligned}$$

We note that  $\Sigma U_{d-1} = U_{d-1} \Lambda_{d-1}$  and  $U_{d-1}^\top \Sigma = \Lambda_{d-1} U_{d-1}^\top$  and hence

$$\begin{aligned}\gamma &= \delta^\top \Sigma \delta - \delta^\top \Sigma U_{d-1} \Lambda_{d-1}^{-1} U_{d-1}^\top \Sigma \delta = \delta^\top \Sigma \delta - \delta^\top U_{d-1} \Lambda_{d-1} \Lambda_{d-1}^{-1} \Lambda_{d-1} U_{d-1}^\top \delta \\ &= \delta^\top \Sigma \delta - \delta^\top U_{d-1} \Lambda_{d-1} U_{d-1}^\top \delta = \delta^\top (\Sigma - \Sigma_{d-1}) \delta\end{aligned}$$

where  $\Sigma_{d-1} = U_{d-1} \Lambda_{d-1} U_{d-1}^\top$  is the best rank  $d - 1$  approximation to  $\Sigma$  with respect to any unitarily invariant norm. In addition,

$$\Lambda_{d-1}^{-1} U_{d-1}^\top \Sigma \delta \delta^\top \Sigma U_{d-1} \Lambda_{d-1}^{-1} = \Lambda_{d-1}^{-1} \Lambda_{d-1} U_{d-1}^\top \delta \delta^\top U_{d-1} \Lambda_{d-1} \Lambda_{d-1}^{-1} = U_{d-1}^\top \delta \delta^\top U_{d-1}.$$

We thus have

$$(A \Sigma A^\top)^{-1} = \begin{bmatrix} \gamma^{-1} & -\delta^\top \Sigma U_{d-1} \Lambda_{d-1}^{-1} \gamma^{-1} \\ -\Lambda_{d-1}^{-1} U_{d-1}^\top \Sigma \delta \gamma^{-1} & (\Lambda_{d-1} - \frac{U_{d-1}^\top \Sigma \delta \delta^\top \Sigma U_{d-1}}{\delta^\top \Sigma \delta})^{-1} \end{bmatrix} = \begin{bmatrix} \gamma^{-1} & -\gamma^{-1} \delta^\top U_{d-1} \\ -\gamma^{-1} U_{d-1}^\top \delta & \Lambda_{d-1}^{-1} + \gamma^{-1} U_{d-1}^\top \delta \delta^\top U_{d-1} \end{bmatrix}.$$

Therefore,

$$\begin{aligned}\delta^\top A^\top (A \Sigma A^\top)^{-1} A \delta &= \delta^\top [\delta \mid U_{d-1}] \begin{bmatrix} \gamma^{-1} & -\gamma^{-1} \delta^\top U_{d-1} \\ -\gamma^{-1} U_{d-1}^\top \delta & \Lambda_{d-1}^{-1} + \gamma^{-1} U_{d-1}^\top \delta \delta^\top U_{d-1} \end{bmatrix} [\delta \mid U_{d-1}]^\top \delta \\ &= [\delta^\top \delta \mid \delta^\top U_{d-1}] \begin{bmatrix} \gamma^{-1} & -\gamma^{-1} \delta^\top U_{d-1} \\ -\gamma^{-1} U_{d-1}^\top \delta & \Lambda_{d-1}^{-1} + \gamma^{-1} U_{d-1}^\top \delta \delta^\top U_{d-1} \end{bmatrix} \begin{bmatrix} \delta^\top \delta \\ U_{d-1}^\top \delta \end{bmatrix} \\ &= \gamma^{-1} (\delta^\top \delta)^2 - 2\gamma^{-1} \delta^\top \delta \delta^\top U_{d-1} U_{d-1}^\top \delta + \delta^\top U_{d-1} (\Lambda_{d-1}^{-1} + \gamma^{-1} U_{d-1}^\top \delta \delta^\top U_{d-1}) U_{d-1}^\top \delta \\ &= \gamma^{-1} (\delta^\top \delta - \delta^\top U_{d-1} U_{d-1}^\top \delta)^2 + \delta^\top U_{d-1} \Lambda_{d-1}^{-1} U_{d-1}^\top \delta \\ &= \gamma^{-1} (\delta^\top (I - U_{d-1} U_{d-1}^\top) \delta)^2 + \delta^\top \Sigma_{d-1}^\dagger \delta\end{aligned}$$

where  $\Sigma_{d-1}^\dagger$  is the Moore-Penrose pseudo-inverse of  $\Sigma_{d-1}$ . The PCA projection matrix into  $\mathbb{R}^d$  is given by  $B = U_d^\top$  and hence

$$\delta^\top B^\top (B \Sigma B^\top)^{-1} B \delta = \delta^\top U_d \Lambda_d^{-1} U_d^\top \delta = \delta^\top \Sigma_d^\dagger \delta. \quad (12)$$

We thus have

$$\begin{aligned}C(F_0^{(A)}, F_1^{(A)}) - C(F_0^{(B)}, F_1^{(B)}) &= \gamma^{-1} (\delta^\top (I - U_{d-1} U_{d-1}^\top) \delta)^2 - \delta^\top (\Sigma_d^\dagger - \Sigma_{d-1}^\dagger) \delta \\ &= \frac{(\delta^\top (I - U_{d-1} U_{d-1}^\top) \delta)^2}{\delta^\top (\Sigma - \Sigma_{d-1}) \delta} - \delta^\top (\Sigma_d^\dagger - \Sigma_{d-1}^\dagger) \delta \\ &\geq \frac{(\delta^\top (I - U_{d-1} U_{d-1}^\top) \delta)^2}{\lambda_d \delta^\top (I - U_{d-1} U_{d-1}^\top) \delta} - \frac{1}{\lambda_d} \delta^\top u_d u_d^\top \delta \\ &= \frac{1}{\lambda_d} \delta^\top (I - U_{d-1} U_{d-1}^\top) \delta - \frac{1}{\lambda_d} \delta^\top (U_d U_d^\top - U_{d-1} U_{d-1}^\top) \delta \geq 0\end{aligned}$$

where we recall that  $u_d$  is the  $d$ -th column of  $U_d$ . Thus  $C(F_0^{(A)}, F_1^{(A)}) \geq C(F_0^{(B)}, F_1^{(B)})$  always, and the inequality is strict whenever  $\delta^\top (I - U_d U_d^\top) \delta > 0$ .  $\square$

**Remark 1.** Theorem 1 can be extended to the case wherein the linear transformations are  $A = [\delta \mid U_{d-1}]$  and  $B = U_d$ , respectively, such that  $U_d$  is an arbitrary  $p \times d$  matrix with  $U_d^\top U_d = I$ , and  $U_{d-1}$  is the first  $d - 1$  columns of  $U_d$ . A similar derivation to that in the proof of Theorem 1 then yields

$$C(F_0^{(A)}, F_1^{(A)}) = \frac{(\delta^\top \Sigma^{-1/2} (I - V_{d-1} V_{d-1}^\top) \Sigma^{1/2} \delta)^2}{\delta^\top \Sigma^{1/2} (I - V_{d-1} V_{d-1}^\top) \Sigma^{1/2} \delta} + \delta^\top \Sigma^{-1/2} V_{d-1} V_{d-1}^\top \Sigma^{-1/2} \delta \quad (13)$$

$$C(F_0^{(B)}, F_1^{(B)}) = \delta^\top \Sigma^{-1/2} V_d V_d^\top \Sigma^{-1/2} \delta \quad (14)$$

where  $V_d V_{d-1}^\top = \Sigma^{1/2} U_d (U_d^\top \Sigma U_d)^{-1} U_d^\top \Sigma^{1/2}$  is the orthogonal projection onto the column space of  $\Sigma^{1/2} U_d$ . Hence  $C(F_0^{(A)}, F_1^{(A)}) > C(F_0^{(B)}, F_1^{(B)})$  if and only if

$$\frac{(\delta^\top \Sigma^{-1/2} (I - V_{d-1} V_{d-1}^\top) \Sigma^{1/2} \delta)^2}{\delta^\top \Sigma^{1/2} (I - V_{d-1} V_{d-1}^\top) \Sigma^{1/2} \delta} > \delta^\top \Sigma^{-1/2} (V_d V_d^\top - V_{d-1} V_{d-1}^\top) \Sigma^{-1/2} \delta. \quad (15)$$

We recover Eq. 11 by letting  $U_d$  be the matrix whose columns are the eigenvectors corresponding to the  $d$  largest eigenvalue of  $\Sigma$ .

We next present a result relating the Chernoff information for LOL and PCA.

**Theorem 2.** Assume the setting of Theorem 1. Let  $C = \tilde{U}_d^\top$  where  $\tilde{U}_d$  is the  $p \times d$  matrix whose columns are the  $d$  largest eigenvectors of the pooled covariance matrix  $\tilde{\Sigma} = \mathbb{E}[(X - \frac{\mu_0 + \mu_1}{2})(X - \frac{\mu_0 + \mu_1}{2})^\top]$ . Then  $C$  is the linear transformation for PCA and

$$\begin{aligned} C(F_0^{(A)}, F_1^{(A)}) - C(F_0^{(C)}, F_1^{(C)}) &= \frac{(\delta^\top (I - U_{d-1} U_{d-1}^\top) \delta)^2}{\delta^\top (\Sigma - \Sigma_{d-1}) \delta} + \delta^\top \Sigma_{d-1}^\dagger \delta - \delta^\top \tilde{\Sigma}_d^\dagger \delta - \frac{(\delta^\top \tilde{\Sigma}_d^\dagger \delta)^2}{4 - \delta^\top \tilde{\Sigma}_d^\dagger \delta} \\ &= \frac{(\delta^\top (I - U_{d-1} U_{d-1}^\top) \delta)^2}{\delta^\top (\Sigma - \Sigma_{d-1}) \delta} + \delta^\top \Sigma_{d-1}^\dagger \delta - \frac{4\delta^\top \tilde{\Sigma}_d^\dagger \delta}{4 - \delta^\top \tilde{\Sigma}_d^\dagger \delta}. \end{aligned} \quad (16)$$

where  $\tilde{\Sigma}_d = \tilde{U}_d \tilde{S}_d \tilde{U}_d^\top$  is the best rank  $d$  approximation to  $\tilde{\Sigma} = \Sigma + \frac{1}{4} \delta \delta^\top$ .

*Proof.* Assume, without loss of generality, that  $\mu_1 = -\mu_0 = \mu$ . We then have

$$\tilde{\Sigma} = \mathbb{E}[X X^\top] = \pi \Sigma + \pi \mu_0 \mu_0^\top + (1 - \pi) \Sigma + (1 - \pi) \mu_1 \mu_1^\top = \Sigma + \mu \mu^\top = \Sigma + \frac{1}{4} \delta \delta^\top.$$

Therefore

$$(C \Sigma C^\top)^{-1} = (\tilde{U}_d^\top \Sigma \tilde{U}_d)^{-1} = (\tilde{U}_d^\top (\tilde{\Sigma} - \frac{1}{4} \delta \delta^\top) \tilde{U}_d)^{-1} = (\tilde{S}_d - \frac{1}{4} \tilde{U}_d^\top \delta \delta^\top \tilde{U}_d)^{-1} = \tilde{S}_d^{-1} + \frac{\tilde{S}_d^{-1} \tilde{U}_d^\top \delta \delta^\top \tilde{U}_d \tilde{S}_d^{-1}}{4 - \delta^\top \tilde{U}_d \tilde{S}_d^{-1} \tilde{U}_d^\top \delta}$$

where  $\tilde{S}_d$  is the diagonal matrix containing the  $d$  largest eigenvalues of  $\tilde{\Sigma}$ . Hence

$$\begin{aligned} C(F_0^{(C)}, F_1^{(C)}) &= \delta^\top C^\top (C \Sigma C^\top)^{-1} C \delta = \delta^\top \tilde{U}_d \left( \tilde{S}_d^{-1} + \frac{\tilde{S}_d^{-1} \tilde{U}_d^\top \delta \delta^\top \tilde{U}_d \tilde{S}_d^{-1}}{4 - \delta^\top \tilde{U}_d \tilde{S}_d^{-1} \tilde{U}_d^\top \delta} \right) \tilde{U}_d^\top \delta \\ &= \delta^\top \tilde{U}_d \tilde{S}_d^{-1} \tilde{U}_d^\top \delta + \frac{(\delta^\top \tilde{U}_d \tilde{S}_d^{-1} \tilde{U}_d^\top \delta)^2}{4 - \delta^\top \tilde{U}_d \tilde{S}_d^{-1} \tilde{U}_d^\top \delta} \\ &= \delta^\top \tilde{\Sigma}_d^\dagger \delta + \frac{(\delta^\top \tilde{\Sigma}_d^\dagger \delta)^2}{4 - \delta^\top \tilde{\Sigma}_d^\dagger \delta} = \frac{4\delta^\top \tilde{\Sigma}_d^\dagger \delta}{4 - \delta^\top \tilde{\Sigma}_d^\dagger \delta}. \end{aligned} \quad (17)$$

as desired.  $\square$

**Remark 2.** We recall that the LOL projection  $A = [\delta \mid U_{d-1}]^\top$  yields

$$C(F_0^{(A)}, F_1^{(A)}) = \frac{(\delta^\top (I - U_{d-1} U_{d-1}^\top) \delta)^2}{\delta^\top (\Sigma - \Sigma_{d-1}) \delta} + \delta^\top \Sigma_{d-1}^\dagger \delta.$$

To illustrate the difference between the LOL projection and that based on the eigenvectors of the pooled covariance matrix, consider the following simple example. Let  $\Sigma = \text{diag}(\lambda_1, \lambda_2, \dots, \lambda_p)$  be a diagonal

matrix with  $\lambda_1 \geq \lambda_2 \geq \dots \geq \lambda_p$ . Also let  $\delta = (0, 0, \dots, 0, s)$ . Suppose furthermore that  $\lambda_p + s^2/4 < \lambda_d$ . Then we have  $\tilde{\Sigma}_d = \text{diag}(\lambda_1, \lambda_2, \dots, \lambda_d, 0, 0, \dots, 0)$ . Thus  $\tilde{\Sigma}_d^\dagger = \text{diag}(1/\lambda_1, 1/\lambda_2, \dots, 1/\lambda_d, 0, 0, \dots, 0)$  and  $\delta^\dagger \tilde{\Sigma}_d^\dagger \delta = 0$ . Therefore,  $C(F_0^{(B)}, F_1^{(B)}) = 0$ .

On the other hand, we have

$$C(F_0^{(A)}, F_1^{(A)}) = \frac{(\delta^\top (I - U_{d-1} U_{d-1}^\top) \delta)^2}{\delta^\top (\Sigma - \Sigma_{d-1}) \delta} + \delta^\top \Sigma_{d-1}^\dagger \delta = \frac{s^4}{s^2 \lambda_p} + 0 = s^2 / \lambda_p.$$

A more general form of the previous observation is the following result which shows that LOL is preferable over PCA when the dimension  $p$  is sufficiently large.

**Proposition 1.** Let  $\Sigma$  be a  $p \times p$  covariance matrix of the form

$$\Sigma = \begin{bmatrix} \Sigma_d & 0 \\ 0 & \Sigma_d^\perp \end{bmatrix}$$

where  $\Sigma_d$  is a  $d \times d$  matrix. Let  $\lambda_1 \geq \lambda_2 \geq \dots \geq \lambda_p$  be the eigenvalues of  $\Sigma$ , with  $\lambda_1, \lambda_2, \dots, \lambda_d$  being the eigenvalues of  $\Sigma_d$ . Suppose that the entries of  $\delta$  are i.i.d. with the following properties.

1.  $\delta_i \sim Y_i * N(\tau, \sigma^2)$  where  $Y_1, Y_2, \dots, Y_p \stackrel{\text{i.i.d.}}{\sim} \text{Bernoulli}(1 - \epsilon)$ .
2.  $p(1 - \epsilon) \rightarrow \theta$  as  $p \rightarrow \infty$  for some constant  $\theta$ .

Then there exists a constant  $C > 0$  such that if  $\lambda_d - \lambda_{d+1} \geq C\theta\tau^2 \log p$ , then, with probability at least  $\epsilon^d$

$$C(F_0^{(A)}, F_1^{(A)}) > C(F_0^{(B)}, F_1^{(B)}) = 0$$

*Proof.* The above construction of  $\Sigma$  and  $\delta$  implies, with probability at least  $\epsilon^d$ , that the covariance matrix for  $\tilde{\Sigma}$  is of the form

$$\tilde{\Sigma} = \begin{bmatrix} \Sigma_d & 0 \\ 0 & \Sigma_d^\perp + \frac{1}{4}(\tilde{\delta}\tilde{\delta}^\top) \end{bmatrix}$$

where  $\tilde{\delta} \in \mathbb{R}^{p-d}$  is formed by excluding the first  $d$  elements of  $\delta$ . Now, if  $\lambda_{d+1} + \frac{1}{4}\|\tilde{\delta}\|^2 < \lambda_d$ , then the  $d$  largest eigenvalues of  $\tilde{\Sigma}$  are still  $\lambda_1, \lambda_2, \dots, \lambda_d$ , and thus the eigenvectors corresponding to the  $d$  largest eigenvalues of  $\tilde{\Sigma}$  are the same as those for the  $d$  largest eigenvalues of  $\Sigma$ . That is to say,

$$\lambda_{d+1} + \frac{1}{4}\|\tilde{\delta}\|^2 < \lambda_d \implies \tilde{\Sigma}_d^\dagger = \Sigma_d^\dagger \implies \delta^\top \tilde{\Sigma}_d^\dagger \delta = 0 \implies C(F_0^{(B)}, F_1^{(B)}) = 0.$$

We now compute the probability that  $\lambda_{d+1} + \frac{1}{4}\|\tilde{\delta}\|^2 < \lambda_d$ . Suppose for now that  $\epsilon > 0$  is fixed and does not vary with  $p$ . We then have

$$\frac{\sum_{i=d+1}^p \delta_i^2 - (p-d)(1-\epsilon)\tau^2}{\sqrt{(p-d)(2(1-\epsilon)(2\tau^2\sigma^2 + \sigma^4) + \epsilon(1-\epsilon)(\tau^4 + 2\tau^2\sigma^2 + \sigma^4))}} \xrightarrow{d} N(0, 1).$$

Thus, as  $p \rightarrow \infty$ , the probability that  $\lambda_{d+1} + \frac{1}{4}\|\tilde{\delta}\|^2 < \lambda_d$  converges to that of

$$\Phi\left(\frac{4(\lambda_d - \lambda_{d+1}) - (p-d)(1-\epsilon)\tau^2}{\sqrt{(p-d)(2(1-\epsilon)(2\tau^2\sigma^2 + \sigma^4) + \epsilon(1-\epsilon)(\tau^4 + 2\tau^2\sigma^2 + \sigma^4))}}\right).$$

This probability can be made arbitrarily close to 1 provided that  $\lambda_d - \lambda_{d+1} \geq Cp(1 - \epsilon)\tau^2$  for all sufficiently large  $p$  and for some constant  $C > 1/4$ . Since the probability that  $\delta_1 = \delta_2 = \dots = \delta_d$  is at least  $\epsilon^d$ , we thus conclude that for sufficiently large  $p$ , with probability at least  $\epsilon^d$ ,

$$C(F_0^{(B)}, F_1^{(B)}) = 0 < C(F_0^{(A)}, F_1^{(A)}).$$

In the case where  $\epsilon = \epsilon(p) \rightarrow 1$  as  $p \rightarrow \infty$  such that  $p(1 - \epsilon) \rightarrow \theta$  for some constant  $\theta$ , then the probability that  $\lambda_{d+1} + \frac{1}{4}\|\delta\|^2 < \lambda_d$  converges to the probability that

$$\frac{1}{4} \sum_{i=1}^K \sigma^2 \chi_1^2(\tau) \geq \lambda_d - \lambda_{d+1}$$

where  $K$  is Poisson distributed with mean  $\theta$  and  $\chi_i^2(\tau)$  is the non-central chi-square distribution with one degree of freedom and non-centrality parameter  $\tau$ . Thus if  $\lambda_d - \lambda_{d+1} \geq C\theta\tau^2 \log p$  for sufficiently large  $p$  and for some constant  $C$ , then this probability can also be made arbitrarily close to 1.  $\square$

## IV.C Finite Sample Performance

We now consider the finite sample performance of LOL and PCA-based classifiers in the high-dimensional setting with small or moderate sample sizes, e.g., when  $p$  is comparable to  $n$  or when  $n \ll p$ . Once again we assume that  $X|Y = i \sim \mathcal{N}(\mu_i, \Sigma)$  for  $i = 0, 1$ . Furthermore, we also assume that  $\Sigma$  belongs to the class  $\Theta(p, r, k, \tau, \lambda)$  as defined below.

**Definition** Let  $\lambda > 0$ ,  $\tau \geq 1$  and  $k \leq p$  be given. Denote by  $\Theta(p, r, k, \tau, \lambda, \sigma^2)$  the collection of matrices  $\Sigma$  such that

$$\Sigma = V\Lambda V^\top + \sigma^2 I$$

where  $V$  is a  $p \times r$  matrix with orthonormal columns and  $\Lambda$  is a  $r \times r$  diagonal matrix whose diagonal entries  $\lambda_1, \lambda_2, \dots, \lambda_r$  satisfy  $\lambda \geq \lambda_1 \geq \lambda_2 \geq \dots \geq \lambda_r \geq \lambda/\tau$ . In addition, assume also that  $|\text{supp}(V)| \leq k$  where  $\text{supp}(V)$  denote the non-zero rows of  $V$ , i.e.,  $\text{supp}(V)$  is the subset of  $\{1, 2, \dots, p\}$  such that  $V_j \neq 0$  if and only if  $j \in \text{supp}(V)$ .

We note that in general  $r \leq k \ll p$  and  $\lambda/\tau \gg \sigma^2$ . We then have the following result.

**Theorem 3** ([58]). Suppose there exist constants  $M_0$  and  $M_1$  such that  $M_1 \log p \geq \log n \geq M_0 \log \lambda$ . Then there exists a constant  $c_0 = c_0(M_0, M_1)$  depending on  $M_0$  and  $M_1$  such that for all  $n$  and  $p$  for which

$$\frac{\tau k}{n} \log \frac{ep}{k} \leq c_0,$$

there exists an estimate  $\hat{V}$  of  $V$  such that

$$\sup_{\Sigma \in \Theta(p, r, k, \tau, \lambda, \sigma^2)} \mathbb{E} \|\hat{V}\hat{V}^\top - VV^\top\|^2 \leq \frac{Ck(\sigma\lambda + \sigma^2)}{n\lambda^2} \log \frac{ep}{k} \quad (18)$$

where  $C$  is a universal constant not depending on  $p, r, k, \tau, \lambda$  and  $\sigma^2$ .

Theorem 3 then implies the following result for comparing the Chernoff information of the sample version of LOL against that for PCA.

**Corollary 4.** Let  $\Sigma \in \Theta(p, r, k, \tau, \lambda)$  as defined above. Suppose that  $C(F_0^{(A)}, F_1^{(A)}) > C(F_0^{(B)}, F_1^{(B)})$  where  $A$  and  $B$  denote the LOL and PCA projection matrices based on the eigenvectors of  $\Sigma$  associated with the  $d \leq r$  largest eigenvalues, i.e,  $A = [\delta|V_{1:d-1}]$  and  $B = V_{1:d}$ . Then there exists constants  $M$  and  $c$  such that if  $\log n \geq M \log \lambda$  and  $\frac{\tau k}{n} \log \frac{ep}{k} \leq c$ , then there exists an estimate  $\hat{V}$  of  $V$  such that, with  $\hat{A} = [\hat{\delta}|\hat{V}_{1:d-1}]$  and  $\hat{B} = [\hat{V}_{1:d}]$ , we have

$$\mathbb{E}[C(F_0^{(\hat{A})}, F_1^{(\hat{A})})] > \mathbb{E}[C(F_0^{(\hat{B})}, F_1^{(\hat{B})})]$$

The above corollary states that for  $\Sigma \in \Theta(p, r, k, \tau, \lambda)$ , then provided that the Chernoff information of the population version of LOL is larger than the Chernoff information of the population version of PCA, we can choose  $n$  sufficiently large (as compared to  $\lambda$  and  $\tau$  and  $k$ ) such that the expected Chernoff information for the sample version of LOL is also larger than the expected Chernoff information of the sample version of PCA. We emphasize that it is necessary that the LOL and the PCA version are both projected into the top  $d \leq r$  dimension of the sample covariance matrices. The constants  $M$  and  $c$  in the statement of the above corollary are chosen so that  $M$  (which depends on  $M_0$  and  $M_1$  in the statement of Theorem 3) is sufficiently large and  $c$  (which depends on  $c_0$ ) is sufficiently small to ensure that the bound in Eq. (18) is sufficiently small. If  $C(F_0^{(A)}, F_1^{(A)}) > C(F_0^{(B)}, F_1^{(B)})$  and  $\|\hat{V}\hat{V}^\top - VV^\top\|$  is sufficiently small, then  $\mathbb{E}[C(F_0^{(\hat{A})}, F_1^{(\hat{A})})] > \mathbb{E}[C(F_0^{(\hat{B})}, F_1^{(\hat{B})})]$  as desired.

#### IV.D Low-rank Canonical Correlation Analysis

We now contrast LOL and low-rank CCA. For discriminant analysis, low-rank CCA corresponds to finding the eigenvectors of  $S_X^\dagger S_B$  where

$$S_X = \sum_i (X_i - \bar{X})(X_i - \bar{X})^\top; \quad \bar{X} = \sum_i X_i$$

is the sample covariance matrix of the  $X_i$ ,  $S_X^\dagger$  is the inverse of  $S_X$  (or Moore-Penrose pseudo-inverse of  $S_X$  if  $S_X$  is not invertible), and

$$S_B = \frac{n_0}{n}(\bar{X}_0 - \bar{X})(\bar{X}_0 - \bar{X})^\top + \frac{n_1}{n}(\bar{X}_1 - \bar{X})(\bar{X}_1 - \bar{X})^\top; \quad \bar{X}_j = \sum_{i: Y_i=j} X_i \text{ for } j \in \{0, 1\}$$

is the between class covariance matrix [7]. It is widely known (see section 11.5 of [59]) that if  $S_X$  is invertible then the above formulation reduces to that of Fisher LDA, namely that of finding  $\hat{v}$  satisfying

$$\hat{v} = \operatorname{argmax}_{v \neq 0} \frac{v^\top S_B v}{v^\top S_W v}$$

$$S_W = \sum_{i: Y_i=0} (X_i - \bar{X}_0)(X_i - \bar{X}_0)^\top + \sum_{i: Y_i=1} (X_i - \bar{X}_1)(X_i - \bar{X}_1)^\top;$$

(here  $S_W$  is the (pooled) within-sample covariance matrix and  $S_X = S_W + S_B$ ). In the context of our current paper where  $X$  is assumed to be high-dimensional, it is well-known that  $S_X$  is not a good estimator of the population covariance matrix  $\Sigma_X = \mathbb{E}[(X - \mu)(X - \mu)^\top]$  and thus computing  $S_X^{-1}$  is suboptimal for subsequent inference unless some form of regularization is employed. Our consideration of low-rank linear transformations  $AX$  provides one principled approach to regularizations of high-dimensional  $S_X$ . In contrast, the above (unregularized) formulation of low-rank CCA frequently yields discrimination direction vectors corresponding to “maximum data piling” (MDP) directions [7, 21]

in high-dimensional settings (and always yield maximum data piling directions when  $n - 1 < p$ ). These MDP directions lead to perfect discrimination of the training data, but can suffer from poor generalization performance, as the examples in [7, 21] indicate.

Finding the  $d$  low-rank CCA vectors, i.e., the eigenvectors of  $S_X^\dagger S_R$  corresponding to the  $d$  largest eigenvalues, is computationally costly, especially when  $n \ll p$ . Denoting by  $U$  the  $p \times d$  matrix whose columns are the naïve computation of  $S_X^\dagger$  requires  $O(p^2)$  storage unless  $X$  is sparse. Efficient implementations of low-rank CCA in the literature circumvent inverting this matrix, but do not circumvent constructing this matrix. For the motivating problems that include  $\mathcal{O}(10^8)$  features, even constructing the  $p^2$  matrix is computationally prohibitive. We therefore devised an approach to implement low-rank CCA without requiring constructing this matrix at all.

In contrast, the dimension-reduced vectors  $U^\top X_i \in \mathbb{R}^d$ ,  $i = 1, 2, \dots, n$  are the rows of the matrix  $M = [m_1 \mid m_2 \cdots \mid m_d]$  whose columns  $m_1, m_2, \dots, m_d$  satisfy the eigenvector problem (see Eq. (7) in [60])

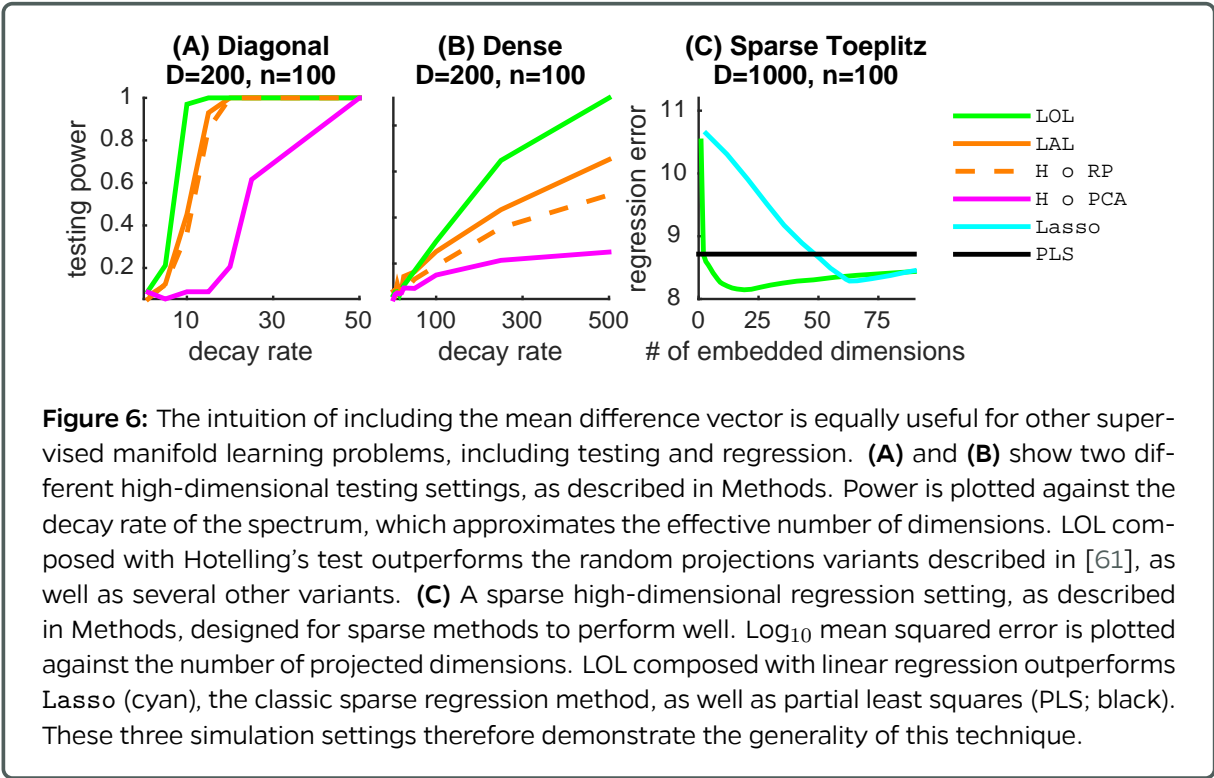
$$\frac{1}{n_1} X(X^\top X)^\dagger X^\top Y Y^\top m_j = \lambda_j m_j.$$

Recalling that  $X(X^\top X)^\dagger X^\top$  is the unique  $n \times n$  (orthogonal) projection matrix onto the column space of  $X$ , we have, by the singular value decomposition of  $X = V_X D_X W_X^\top$  that  $X(X^\top X)^\dagger X^\top = V_X V_X^\top$  where  $V_X$  is the  $n \times n$  matrix whose columns are the left singular vectors of  $X$ . This approach requires  $O(n^2)$  storage. We emphasize that the approach only yield the transformed vectors  $U^\top X_i$  and not the transformation matrix  $U$  itself.

## E Extensions to Other Supervised Learning Problems

The utility of incorporating the mean difference vector into supervised machine learning extends beyond classification. In particular, hypothesis testing can be considered as a special case of classification, with a particular loss function. We therefore apply the same idea to a hypothesis testing scenario. The multivariate generalization of the t-test, called Hotelling’s Test, suffers from the same problem as does the classification problem; namely, it requires inverting an estimate of the covariance matrix, which would result in a matrix that is low-rank and therefore singular in the high-dimensional setting. To mitigate this issue in the hypothesis testing scenario, prior work applied similar tricks as they have done in the classification setting. One particularly nice and related example is that of Lopes et al. [61], who addresses this dilemma by using random projections to obtain a low-dimensional representation, following by applying Hotelling’s Test in the lower-dimensional subspace. Figure 6A and B show the power of their test (labeled RP) alongside the power of PCA, LOL, and LFL for two different conditions. In each case we use the different approaches to project to low dimensions, followed by using Hotelling’s test on the projected data. In the first example the true covariance matrix is diagonal, and in the second, the true covariance matrix is dense. The horizontal axis on both panels characterizes the decay rate of the eigenvalues, so larger numbers imply the data is closer to low-rank (see Methods for details). The results indicate that the LOL test has higher power for essentially all scenarios. Moreover, it is not merely replacing random projections with PCA (solid magenta line), nor simply incorporating the mean difference vector (dashed green line), but rather, it appears that LOL for testing uses both modifications to improve performance.

High-dimensional regression is another supervised learning method that can use the LOL idea. Linear regression, like classification and Hotelling’s Test, requires inverting a matrix as well. By projecting the data onto a lower-dimensional subspace first, followed by linear regression on the low-dimensional



data, we can mitigate the curse of high-dimensions. To choose the projection matrix, we partition the data into  $K$  partitions, based on the percentile of the target variable, we obtain a  $K$ -class classification problem. Then, we can apply LOL to learn the projection. Figure 6C shows an example of this approach, contrasted with Lasso and partial least squares, in a sparse simulation setting (see Methods for details). LOL is able to find a better low-dimensional projection than Lasso, and performs significantly better than partial least squares, for essentially all choices of number of dimensions to project into.

## F The R implementation of LOL

Figure 7 shows the R implementation of LOL for binary classification using FlashMatrix [25]. The implementation takes a  $D \times I$  matrix, where each column is a training instance and each instance has  $D$  features, and outputs a  $D \times k$  projection matrix.

```

LOL <- function(m, labels, k) {
  counts <- fm.table(labels)
  num.labels <- length(counts$val)
  num.features <- dim(m)[1]
  nv <- k - (num.labels - 1)
  gr.sum <- fm.groupby(m, 1, fm.as.factor(labels, 2), fm.bo.add)
  gr.mean <- fm.mapply.row(gr.sum, counts$Freq, fm.bo.div, FALSE)
  diff <- fm.get.cols(gr.mean, 1) - fm.get.cols(gr.mean, 2)
  svd <- fm.svd(m, nv=0, nu=nv)
  fm.cbind(diff, svd$u)
}

```

Figure 7: The R implementation of LOL.

---

**Pseudocode 1** Simple pseudocode for two class LOL on sample data.

---

**Input:**  $X$  a  $p \times n$  matrix ( $n \ll p$ ), where columns are observations; rows are features. An  $n$  length vector of observation labels,  $\mathbf{y}$ . An integer  $k$  to specify desired output dimension.

**Output:**  $A \in \mathbb{R}^{p \times k}$

```

1: function LOL.TRAIN( $X, Y, k$ )
2:   for all  $j \in J$  do
3:      $n_j = \sum_{i=1}^n \mathbf{I}(y_i = j)$  ▷ sample size per class
4:      $\hat{\mu}_j = \frac{1}{n_j} \sum_{i=1}^n \mathbf{x}_i \mathbf{I}(y_i = j)$  ▷ class means
5:   end for
6:    $\hat{\delta} = \hat{\mu}_1 - \hat{\mu}_2$  ▷ difference of means
7:    $\hat{\delta} = \hat{\delta} / \|\hat{\delta}\|$  ▷ unit normalize difference of means
8:   for all  $i \in [n]$  do
9:      $\tilde{\mathbf{x}}_i = \mathbf{x}_i - \hat{\mu}_{y_i}$  ▷ class centered data
10:  end for
11:   $[\hat{u}, \hat{d}, \hat{v}] = \text{svds}(\tilde{\mathbf{x}}, k - 1)$  ▷ compute top  $k$  singular vectors
12:   $A = [\hat{\delta}, \hat{u}]$  ▷ concatenate difference of the means and the top  $k$  right singular vectors
13: end function

```

---

## Bibliography

- [1] J. T. Vogelstein, Y. Park, T. Ohshima, R. Kerr, J. Truman, C. E. Priebe, and M. Zlatić, “Discovery of brainwide neural-behavioral maps via multiscale unsupervised structure learning,” *Science*, vol. 344, no. 6182, pp. 386–392, 2014. [1](#)
- [2] A. Krizhevsky, I. Sutskever, and G. E. Hinton, “ImageNet Classification with Deep Convolutional Neural Networks,” in *Advances in Neural Information Processing Systems*, 2012, pp. 1097–1105. [Online]. Available: <http://papers.nips.cc/paper/4824-imagenet-classification-w> [1](#)
- [3] R. A. Fisher, “Theory of Statistical Estimation,” *Mathematical Proceedings of the Cambridge Philosophical Society*, vol. 22, no. 05, pp. 700–725, Oct. 1925. [Online]. Available: [http://journals.cambridge.org/abstract\\_S0305004100009580](http://journals.cambridge.org/abstract_S0305004100009580) [1](#)
- [4] I. T. Jolliffe, “Principal component analysis and factor analysis,” in *Principal Component Analysis*, ser. Springer Series in Statistics. Springer, New York, NY, 1986, pp. 115–128. [1](#)
- [5] J. A. Lee and M. Verleysen, *Nonlinear Dimensionality Reduction (Information Science and Statistics)*, 2007th ed. Springer, Dec. 2007. [2](#)
- [6] D. M. Witten and R. Tibshirani, “Covariance-regularized regression and classification for high-dimensional problems.” *Journal of the Royal Statistical Society. Series B, Statistical methodology*, vol. 71, no. 3, pp. 615–636, Feb. 2009. [Online]. Available: <http://www.pubmedcentral.nih.gov/articlerender.fcgi?artid=2806603&tool=pmcentrez&rendertype=abstract> [2](#)
- [7] H. Shin and R. L. Eubank, “Unit canonical correlations and high-dimensional discriminant analysis,” *Journal of Statistical Computation and Simulation*, vol. 81, pp. 167–178, 2011. [2](#), [27](#), [28](#)
- [8] T. Hastie, R. Tibshirani, and M. Wainwright, *Statistical Learning with Sparsity: The Lasso and Generalizations (Chapman & Hall/CRC Monographs on Statistics & Applied Probability)*, 1st ed. Chapman and Hall/CRC, may 2015. [2](#)
- [9] R. Tibshirani, “Regression Shrinkage and Selection via the Lasso,” *Journal of the Royal Statistical Society. Series B*, vol. 58, pp. 267–288, 1996. [2](#)
- [10] W. Su, M. Bogdan, and E. Candes, “False discoveries occur early on the lasso path,” *arXiv*, nov 2015. [2](#)
- [11] J. Fan, Y. Feng, and X. Tong, “A road to classification in high dimensional space: the regularized optimal affine discriminant,” *Journal of the Royal Statistical Society: Series B (Statistical Methodology)*, vol. 74, no. 4, pp. 745–771, Sep. 2012. [Online]. Available: <http://doi.wiley.com/10.1111/j.1467-9868.2012.01029.x> [2](#), [6](#), [7](#)
- [12] A. Agarwal, O. Chapelle, M. Dudík, and J. Langford, “A reliable effective terascale linear learning system,” *J. Mach. Learn. Res.*, vol. 15, pp. 1111–1133, 2014. [2](#), [12](#)
- [13] M. Abadi, A. Agarwal, P. Barham, E. Brevdo, Z. Chen, C. Citro, G. S. Corrado, A. Davis, J. Dean, M. Devin et al., “Tensorflow: Large-scale machine learning on heterogeneous distributed systems,” *arXiv preprint arXiv:1603.04467*, 2016. [2](#)
- [14] Y. LeCun, C. Cortes, and C. Burges, “MNIST handwritten digit database.” [Online]. Available: <http://yann.lecun.com/exdb/mnist/> [3](#)

- [15] Y. Bengio, J.-F. Paiement, P. Vincent, O. Delalleau, N. L. Roux, and M. Ouimet, “Out-of-Sample extensions for LLE, isomap, MDS, eigenmaps, and spectral clustering,” in *Advances in Neural Information Processing Systems 16*, S. Thrun, L. K. Saul, and P. B. Schölkopf, Eds. MIT Press, 2004, pp. 177–184. [3](#)
- [16] P. J. Bickel and E. Levina, “Some theory for Fisher’s linear discriminant function, ‘naive Bayes’, and some alternatives when there are many more variables than observations,” *Bernoulli*, vol. 10, no. 6, pp. 989–1010, Dec. 2004. [Online]. Available: <http://projecteuclid.org/euclid.bj/1106314847> [4](#)
- [17] T. Hastie and R. Tibshirani, “Discriminant analysis by gaussian mixtures,” *J. R. Stat. Soc. Series B Stat. Methodol.*, vol. 58, no. 1, pp. 155–176, 1996. [4](#)
- [18] H. Chernoff, “A measure of asymptotic efficiency for tests of a hypothesis based on the sum of observations,” *Annals of Mathematical Statistics*, vol. 23, pp. 493–507, 1952. [6](#), [20](#)
- [19] H. Zou, “The Adaptive Lasso and Its Oracle Properties,” pp. 1418–1429, 2006. [7](#)
- [20] T. Hastie, R. Tibshirani, and J. H. Friedman, “The Elements of Statistical Learning: Data Mining, Inference, and Prediction,” BeiJing: Publishing House of Electronics Industry, 2004. [7](#)
- [21] J. Ahn and J. S. Marron, “The maximum data piling direction for discrimination,” *Biometrika*, vol. 97, pp. 254–259, 2010. [9](#), [27](#), [28](#)
- [22] J. Mairal, J. Ponce, G. Sapiro, A. Zisserman, and F. R. Bach, “Supervised Dictionary Learning,” in *Advances in Neural Information Processing Systems*, 2009, pp. 1033–1040. [Online]. Available: <http://papers.nips.cc/paper/3448-supervised> [9](#), [12](#)
- [23] D. Zheng, D. Mhembere, R. Burns, J. Vogelstein, C. E. Priebe, and A. S. Szalay, “FlashGraph: Processing billion-node graphs on an array of commodity SSDs,” in *13th USENIX Conference on File and Storage Technologies (FAST 15)*, Santa Clara, CA, 2015. [9](#)
- [24] D. Zheng, R. Burns, J. Vogelstein, C. E. Priebe, and A. S. Szalay, “An ssd-based eigensolver for spectral analysis on billion-node graphs,” *CoRR*, vol. abs/1602.01421, 2016.
- [25] D. Zheng, D. Mhembere, J. T. Vogelstein, C. E. Priebe, and R. Burns, “Flashmatrix: Parallel, scalable data analysis with generalized matrix operations using commodity ssds,” *arXiv preprint arXiv:1604.06414*, 2016. [9](#), [30](#)
- [26] E. J. Candès and T. Tao, “Near-Optimal Signal Recovery From Random Projections: Universal Encoding Strategies?” *IEEE Transactions on Information Theory*, vol. 52, no. 12, pp. 5406–5425, dec 2006. [Online]. Available: <http://ieeexplore.ieee.org/lpdocs/epic03/wrapper.htm?arnumber=4016283> [9](#)
- [27] T. Hastie, K. W. Church, P. Li, and K. C. Kdd, “Very sparse random projections,” *Proceedings of the 12th ACM SIGKDD international conference on Knowledge discovery and data mining - KDD '06*, p. 287, 2006. [Online]. Available: <http://portal.acm.org/citation.cfm?doid=1150402.1150436> [9](#)
- [28] W. R. Gray, J. A. Bogovic, J. T. Vogelstein, B. A. Landman, J. L. Prince, and R. J. Vogelstein, “Magnetic resonance connectome automated pipeline,” *IEEE Pulse*, vol. 3, no. 2, pp. 42–48, 2011. [10](#)
- [29] W. Gray Roncal et al., “MIGRAINE: MRI Graph Reliability Analysis and Inference for Connectomics,” *Global Conference on Signal and Information Processing*, 2013.

- [30] G. Kiar, K. J. Gorgolewski, D. Kleissas, W. Gray Roncal, B. Litt, B. Wandell, R. A. Poldrack, M. Wiener, R. Vogelstein, R. Burns, and J. T. Vogelstein, "Science in the cloud (sic): A use case in mri connectomics," *GigaScience*, vol. gix013, mar 2017. 10
- [31] J. T. Vogelstein, W. G. Roncal, R. J. Vogelstein, and C. E. Priebe, "Graph classification using Signal-Subgraphs: Applications in statistical connectomics," *IEEE Trans. Pattern Anal. Mach. Intell.*, vol. 35, no. 7, pp. 1539–1551, 2013. 11
- [32] J. M. Duarte-Carvajalino and N. Jahanshad, "Hierarchical topological network analysis of anatomical human brain connectivity and differences related to sex and kinship," *Neuroimage*, vol. 59, no. 4, pp. 3784–3804, 2011. 11
- [33] R. C. Craddock, S. S. Jbabdi, C.-G. Yan, J. T. Vogelstein, X. F. Castellanos, A. Di Martino, A. M. C. Kelly, K. Heberlein, S. J. Colcombe, M. P. Milham, F. X. Castellanos, A. Di Martino, C. Kelly, K. Heberlein, S. J. Colcombe, M. P. Milham, X. F. Castellanos, A. Di Martino, A. M. C. Kelly, K. Heberlein, S. J. Colcombe, and M. P. Milham, "Imaging functional and structural connectomes at the macroscale," *Nat. Methods*, vol. 10, no. 6, pp. 524–539, 2013. 11
- [34] P. N. Belhumeur, J. P. Hespanha, and D. J. Kriegman, "Eigenfaces vs. fisherfaces: Recognition using class specific linear projection," *IEEE Transactions on Pattern Analysis and Machine Intelligence*, vol. 19, no. 7, pp. 711–720, 1997. 11
- [35] C. Eckart and G. Young, "The approximation of one matrix by another of lower rank," *Psychometrika*, vol. 1, no. 3, pp. 211–218, Sep. 1936. [Online]. Available: <http://www.springerlink.com/content/9v4274h33h75lq24/> 11
- [36] V. de Silva and J. B. Tenenbaum, "Global Versus Local Methods in Nonlinear Dimensionality Reduction," in *Neural Information Processing Systems*, 2003, pp. 721–728.
- [37] W. K. Allard, G. Chen, and M. Maggioni, "Multi-scale geometric methods for data sets II: Geometric Multi-Resolution Analysis," *Applied and Computational Harmonic Analysis*, vol. 32, no. 3, pp. 435–462, May 2012. [Online]. Available: <http://linkinghub.elsevier.com/retrieve/pii/S1063520311000868> 11, 12
- [38] K.-C. Li, "Sliced Inverse Regression for Dimension Reduction," *Journal of the American Statistical Association*, vol. 86, no. 414, pp. 316–327, Jun. 1991. [Online]. Available: <http://www.tandfonline.com/doi/abs/10.1080/01621459.1991.10475035> 12
- [39] N. Tishby, F. C. Pereira, and W. Bialek, "The information bottleneck method arXiv : physics / 0004057v1 [ physics . data-an ] 24 Apr 2000," *Neural Computation*, pp. 1–16, 1999.
- [40] A. Globerson and N. Tishby, "Sufficient Dimensionality Reduction," *Journal of Machine Learning Research*, vol. 3, no. 7-8, pp. 1307–1331, Oct. 2003. [Online]. Available: [http://www.crossref.org/jmlr\\_DOI.html](http://www.crossref.org/jmlr_DOI.html)
- [41] R. D. Cook and L. Ni, "Sufficient Dimension Reduction via Inverse Regression," *Journal of the American Statistical Association*, vol. 100, no. 470, pp. 410–428, Jun. 2005. [Online]. Available: <http://amstat.tandfonline.com/doi/abs/10.1198/016214504000001501#.U6tH3Y1dUts>
- [42] K. Fukumizu, F. R. Bach, and M. I. Jordan, "Dimensionality Reduction for Supervised Learning with Reproducing Kernel Hilbert Spaces," *Journal of Machine Learning Research*, vol. 5, pp. 73–99, 2004. 12

- [43] R. D. Cook, L. Forzani, and A. J. Rothman, "Prediction in abundant high-dimensional linear regression," *Electronic Journal of Statistics*, vol. 7, pp. 3059–3088, 2013. [Online]. Available: <https://projecteuclid.org/euclid.ejs/1387207935> 12
- [44] M. Nokleby, M. Rodrigues, and R. Calderbank, "Discrimination on the grassmann manifold: Fundamental limits of subspace classifiers," *IEEE Trans. Inf. Theory*, vol. 61, no. 4, pp. 2133–2147, Apr. 2015. 12
- [45] P. J. Huber, "Projection Pursuit," *The Annals of Statistics*, vol. 13, no. 2, pp. 435–475, Jun. 1985. [Online]. Available: <http://projecteuclid.org/euclid.aos/1176349519> 12
- [46] M. Belkin, P. Niyogi, and V. Sindhvani, "Manifold Regularization: A Geometric Framework for Learning from Labeled and Unlabeled Examples," *The Journal of Machine Learning Research*, vol. 7, pp. 2399–2434, Dec. 2006. [Online]. Available: <http://dl.acm.org/citation.cfm?id=1248547.1248632><http://dl.acm.org/citation.cfm?id=1248632> 12
- [47] D. L. Donoho and J. Jin, "Higher criticism thresholding: Optimal feature selection when useful features are rare and weak." *Proceedings of the National Academy of Sciences of the United States of America*, vol. 105, no. 39, pp. 14 790–5, Sep. 2008. [Online]. Available: <http://www.pnas.org/content/105/39/14790><http://www.pnas.org/content/105/39/14790.short> 12
- [48] E. Bair, T. Hastie, D. Paul, and R. Tibshirani, "Prediction by supervised principal components," *J. Am. Stat. Assoc.*, vol. 101, no. 473, pp. 119–137, mar 2006. 12
- [49] A. Gretton, R. Herbrich, A. Smola, O. Bousquet, and B. Scholkopf, "Kernel methods for measuring independence," *Journal of Machine Learning Research*, vol. 6, pp. 2075–2129, 2005. 12
- [50] E. Barshan, A. Ghodsi, Z. Azimifar, and M. Zolghadri Jahromi, "Supervised principal component analysis: Visualization, classification and regression on subspaces and submanifolds," *Pattern Recognit.*, vol. 44, no. 7, pp. 1357–1371, jul 2011. 12
- [51] S. Mika, G. Ratsch, J. Weston, B. Scholkopf, and K. Mullers, "Fisher discriminant analysis with kernels," in *Neural Networks for Signal Processing IX: Proceedings of the 1999 IEEE Signal Processing Society Workshop (Cat. No.98TH8468)*. IEEE, 1999, pp. 41–48. [Online]. Available: <http://ieeexplore.ieee.org/lpdocs/epic03/wrapper.htm?arnumber=788121> 12
- [52] T. I. Cannings and R. J. Samworth, "Random-projection ensemble classification," *arXiv*, Apr 2015. 12
- [53] L. Breiman, "Random forests," *Machine learning*, vol. 45, no. 1, pp. 5–32, 2001. 12
- [54] E. Anderson, Z. Bai, C. Bischof, S. Blackford, J. Demmel, J. Dongarra, J. D. Croz, A. Greenbaum, S. Hammerling, A. McKenney, and D. Sorensen, *LAPACK Users' Guide: Third Edition*. SIAM, 1999. [Online]. Available: <https://books.google.com/books?hl=en&lr=&id=AZlvEnr9gCgC&pgis=1> 15
- [55] L. Breiman, "Statistical modeling: The two cultures," *Statistical Science*, vol. 16, no. 3, pp. 199–231, 2001. 17
- [56] I. Csizár, "Information-type measures of difference of probability distributions and indirect observations," *Studia Scientiarum Mathematicarum Hungarica*, vol. 2, pp. 229–318, 1967. 21
- [57] C. C. Leang and D. H. Johnson, "On the asymptotics of M-hypothesis bayesian detection," *IEEE Transactions on Information Theory*, vol. 43, pp. 280–282, 1997. 21

- [58] T. Cai, Z. Ma, and Y. Wu, “Optimal estimation and rank detection for sparse spiked covariance matrices,” *Probab. Theory Related Fields*, vol. 161, no. 3-4, pp. 781–815, apr 2015. 26
- [59] K. V. Mardia, J. T. Kent, and J. M. Bibby, *Multivariate Analysis*. Academic Press, 1979. 27
- [60] M. Kuss and T. Graepel, “The geometry of kernel canonical correlation analysis,” Max Planck Institute for Biological Cybernetics, Tech. Rep. TR-108, 2003. 28
- [61] M. Lopes, L. Jacob, and M. J. Wainwright, “A More Powerful Two-Sample Test in High Dimensions using Random Projection,” in *Neural Information Processing Systems*, 2011, pp. 1206–1214. [Online]. Available: <http://papers.nips.cc/paper/4260-a-more-powerful-two-sample-test-in-high-dimensions-using-random-projection> 28, 29

## Acknowledgements

The authors are grateful for the support by the XDATA program of the Defense Advanced Research Projects Agency (DARPA) administered through Air Force Research Laboratory contract FA8750-12-2-0303; DARPA GRAPHS contract N66001-14-1-4028; and DARPA SIMPLEX program through SPAWAR contract N66001-15-C-4041.